

Variational principle and time-space finite element method for dynamic thermoelasticity based on mixed convolved action

Bradley T. Darrall, Gary F. Dargush*

Department of Mechanical and Aerospace Engineering, University at Buffalo, State University of New York, Buffalo, NY 14260, USA

Abstract

A new variational formulation is proposed for time-domain analysis of initial/boundary value problems of dynamic thermoelasticity. By using the concept of mixed convolved action, the difficulties with dissipative phenomena and proper representations of the temporal end point conditions can be overcome to create a true stationary variational principle. After an elementary illustrative development for a lumped parameter thermoelastic model, the convolved action functional for a linear thermoelastic continua is written directly in terms of mixed variables, which include displacements and the impulses of stress, temperature and heat flux. Unlike previous variational approaches, based for example upon a generalization of Hamilton's principle, the present mixed convolved action formulation allows direct application of finite element methodology in both space and time. Here, simple linear shape functions are employed for the temporal representations. Meanwhile, standard three-noded triangular elements are used in the present two-dimensional numerical implementation. Several computational examples are considered to test this original approach and to investigate interesting aspects of coupled dynamic thermoelastic response.

1. Introduction

The attractiveness of the analytical dynamics branch of mechanics is undeniable. The idea of capturing the essence of a conservative dynamical system in a single scalar functional is compelling. However, the incorporation of dissipative phenomena into this framework has been a significant challenge, ever since the

* Corresponding author. Tel.: 1 716 645 2315.

E-mail addresses: gdargush@buffalo.edu (G.F. Dargush), bdarrall@buffalo.edu (B.T. Darrall)

formulation of Hamilton's principle nearly two centuries ago (Hamilton, 1834, 1835; Lanczos, 1949; Goldstein, 1950). Mirror systems (Morse and Feshbach, 1953), additional dissipation functions (Rayleigh, 1877; Biot, 1955; Marsden and Ratiu, 1994) and fractional derivatives (Riewe, 1996, 1997) have all been proposed as solutions, but these come with shortcomings involving non-physical governing equations, ad hoc variational operations and unproven functionals, respectively. In addition, careful consideration of the underlying assumptions leads to concern, even for conservative systems, because of the treatment of the end point requirements. In particular, one must assume that the variations vanish at both end points of the time interval. Beginning from some known conditions with zero variation at the initial instant is logical, but how can one not vary the end state, when this is most often the object of the dynamic analysis?

In order to overcome both limitations of Hamilton's principle, convolution-based temporal operators are needed. Gurtin (1963, 1964a,b) was the first to advance this concept by introducing functionals containing temporal convolutions to address continuum problems of viscoelasticity and elastodynamics. The subsequent work by Tonti (1973, 1985) in advocating the use of the convolutional bilinear form to replace the usual inner product form of Hamilton's principle was particularly insightful. Afterwards, Oden and Reddy (1983) extended the formulations of both Gurtin and Tonti to a large class of boundary and initial value problems in mechanics, especially for Hellinger-Reissner type mixed principles to provide the governing partial differential equations, boundary conditions and initial conditions as the Euler-Lagrange equations emanating from stationarity of the functional. Their highly original convolution-based formulations cover linear problems of elastodynamics, viscoelasticity, thermoelasticity and piezoelectricity. However, we should mention that for dynamic thermoelasticity, the Oden and Reddy (1983) formulation is limited to a Gurtin-based approach, which produces integro-differential Euler-Lagrange equations, rather than the partial differential equations associated with the standard definition of the problem.

A remaining question is whether one can formulate a single real scalar functional for dissipative systems that captures all of the governing partial differential equations, boundary conditions and initial conditions

of the problem, along with any restrictions on the variations, as its Euler-Lagrange equations? This has been accomplished by introducing the mixed convolved action for single-degree-of-freedom dynamical systems (Dargush and Kim, 2012), elastodynamic continuum systems (Dargush et al., 2015) and for dissipative systems associated with heat diffusion (Dargush et al., 2016). This mixed convolved action framework appears to be quite general with the possibility to extend to a broad range of linear time-invariant systems. Here we address the extension of the mixed convolved action to dynamic thermoelasticity.

Before continuing with this mixed convolved action development, we should mention other important related work for dissipative processes in general and then also outline key theoretical and computational contributions in the field of thermoelasticity. In the former domain, Sivaselvan and Reinhorn (2006) developed the mixed Lagrangian formalism (MLF) for both linear and non-linear structural and continuum mechanics analyses, based upon impulsive variables that bring a useful symmetry to the form of the governing equations. Other work on MLF includes that by Sivaselvan et al. (2009) for plasticity, Lavan et al. (2009, 2010) for contact and fracture, and Apostolakis and Dargush (2012, 2013) for thermoelasticity. Along similar lines, many formulations for dissipative systems have been advanced using extensions of the variational approaches by Halphen and Nguyen Quoc (1975), Brezis and Ekeland (1976) and Nayroles (1976), involving convex, perhaps non-differentiable, stored energy and dissipation functionals. Specific examples in this category include the development by deSaxce and Feng (1998) on friction, and the more recent work on elastoplasticity by Houlsby and Puzrin (2006), Lotfian and Sivaselvan (2014) and Buliga and deSaxce (2017).

An interesting alternative approach uses generalized bracket formalisms to address a broad range of dissipative processes (Kaufman, 1984; Morrison, 1984; Grmela, 1984; Beris and Edwards, 1994; Grmela and Ottinger, 1997; Ottinger and Grmela, 1997). The recent extensions that are provided in Grmela (2014, 2015), and the references cited therein, focus on developing an underlying geometric structure for multi-scale dissipative processes by combining the elements of dynamics and thermodynamics.

Moving next to consider the classical thermoelastic problem, we should perhaps begin with the comprehensive monographs by Boley and Weiner (1960) and Nowacki (1986), which present governing equations, fundamental solutions, integral equations and analytical solutions to a range of boundary/initial value problems. Other notable work includes the foundational development by Biot (1956, 1959) and the dynamic reciprocal theorem of Ionescu-Casimer (1964). Finite element methods were first developed long ago by Gallagher et al. (1962) for stress analysis of heated bodies, Wilson and Nickell (1966) for transient heat conduction and then Nickell and Sackman (1968) for dynamic coupled thermoelasticity.

All of this early work is squarely within the realm of classical thermoelasticity. Consequently, these developments are based upon the Fourier law of heat conduction, which leads to diffusion processes that suffer from a non-physical infinite speed of propagation of thermal impulses. To correct this deficiency, several different generalized thermoelastic theories have been proposed, including those by Lord and Shulman (1967) and Green and Lindsay (1972) involving one and two relaxation times, respectively. The former generalized theory is based upon a modified Fourier law that Chester (1963) associated with second sound phenomena. On the other hand, the latter theory retains the classical Fourier law, modifying instead the Duhamel-Neumann and entropy density constitutive relations. Prevost and Tao (1983) developed a finite element method for the Green and Lindsay (1972) formulation, while in recent work Apostolakis and Dargush (2012, 2013) presented an MLF for thermoelasticity based upon the Chester (1963) heat conduction model. A boundary element method by Chen and Dargush (1995) addressed dynamic problems for both generalized dynamic thermoelastic models in two- and three-dimensions using a boundary-only Laplace transform domain approach. The interesting special case of dissipationless thermoelasticity was considered by Green and Naghdi (1992, 1993). It remains to be seen whether this limit can be approached, while retaining a continuum representation. A comprehensive review of early theoretical, computational and experimental efforts on heat waves is provided by Joseph and Perziosi (1989).

Other more recent work to generalize classical thermoelasticity, includes Ezzat and El-Karamany (2012) on generalized thermoviscoelasticity with two relaxation times, Sherief et al. (2010) on fractional order thermoelasticity, and then a Gurtin-style convolutional variational approach by El-Karamany and Ezzat (2011) for linear fractional thermoelasticity, which extends the two-temperature model advanced by Chen and Gurtin (1968).

Here, in the present paper, we explore the extension of the mixed convolved action to a multi-physics problem involving the coupling between mechanical and thermal fields, which includes both conservative and dissipative elements. Specifically, we address dynamic coupled thermoelastic problems that may also include second sound effects. In the process, we propose a new stationary action principle, based upon impulsive mixed variables, fractional derivatives and convolutions to produce an elegant theoretical structure for linear initial/boundary value problems of generalized thermoelasticity. A novel space-time finite element formulation also is developed to solve these dynamical problems directly in the time domain.

The remainder of the paper is organized as follows. In Section 2 a mixed convolved action principle is formulated for a simplified lumped dynamic thermoelastic system. In Section 3 we provide an overview of the governing equations for a coupled dynamic thermoelastic continuum. Then, in Section 4, we present the stationary mixed convolved action principle for the continuum problem. Based on this principle, we proceed to develop a corresponding finite element formulation over space and time in Section 5. Next, in Section 6, this finite element formulation is applied to solve two illustrative problems of coupled dynamic thermoelasticity. Finally, in Section 7, we present conclusions.

2. Mixed convolved action for lumped thermoelasticity

Before developing relations for the case of thermoelastodynamic continua in the subsequent sections, we first consider here a simplified lumped parameter dynamic thermoelastic system. This lumped system is

depicted in Fig. 1 as a lumped mass m with constant heat capacity c_ε submerged in a bath of constant temperature T_∞ with a single displacement degree of freedom u . Connecting the mass to the presumed rigid wall is a typical linear elastic spring element, and a less commonly used linear thermoelastic element. Here the thermoelastic element is considered highly conductive and insulated from the bath, such that at any time it has the same temperature T as the mass. Let us consider here that T represents the temperature change from a temperature T_o which corresponds to an undeformed state of the thermoelastic element. The system can also generally be exposed to some applied force \bar{f} and body heating $\bar{\psi}$, where the overbar defines a known or specified quantity, not to be subject to any variation.

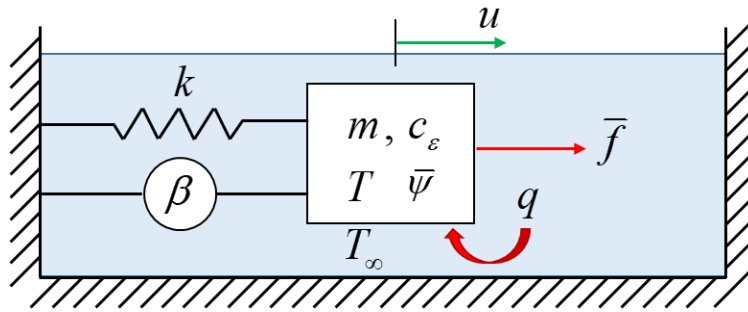


Fig. 1. Lumped parameter thermoelasticity problem

As is done in Apostolakis and Dargush (2012), we define impulsive variables as

$$u(t) = \int_0^t v(t) dt \quad (1a)$$

$$J(t) = \int_0^t f_s(t) dt = \int_0^t k u(t) dt \quad (1b)$$

$$\theta(t) = \int_0^t T(t) dt \quad (1c)$$

$$H(t) = \int_0^t q(t) dt \quad (1d)$$

such that the displacement u is identified as the impulse of the velocity v , J is the impulse of the stored spring force $f_s = ku$, θ is the impulse of the temperature T , and H is the impulse of the heat flux q .

Alternatively, using a dot to represent a single time derivative, we can define these quantities in rate form:

$$\dot{u} = v \quad (2a)$$

$$\dot{J} = f_s = ku \quad (2b)$$

$$\dot{\theta} = T \quad (2c)$$

$$\dot{H} = q \quad (2d)$$

The thermoelastic element under a constrained displacement condition will store an internal force proportional to the coupling coefficient β , such that

$$f_T = -\beta T = -\beta \dot{\theta} \quad (3)$$

The following four equations, written in terms of impulsive variables, and corresponding to Newton's second law, the compatibility in rate form for a linear spring, energy-entropy balance, and Newton's law of cooling, constitute all of the governing equations for this lumped dynamic thermoelastic problem:

$$m\ddot{u} + (\dot{J} - \beta\dot{\theta}) = \dot{\bar{j}} \quad (4a)$$

$$\frac{1}{k}\ddot{J} - \dot{u} = 0 \quad (4b)$$

$$\frac{mc_\epsilon}{T_o}\ddot{\theta} - \frac{1}{T_o}\dot{H} + \beta\dot{u} = \frac{1}{T_o}\dot{\bar{\Psi}} \quad (4c)$$

$$\frac{1}{hAT_o}\dot{H} + \frac{1}{T_o}\dot{\theta} = 0 \quad (4d)$$

where \bar{j} is the impulse of the applied force, $\bar{\Psi}$ is the impulse of the body heat source, h is the convection coefficient, and A is the surface area of the mass. Note that for the sake of keeping the governing equations as similar as possible to the continuum case, (4d) is written assuming that the bath temperature is equal to

T_o , however for any other case (4d) would simply need to be amended by adding to the right hand side the constant term $\frac{1}{T_o}(T_\infty - T_o)$.

At this point in previous papers for lumped parameter systems (Dargush and Kim, 2012; Dargush, 2012), a mixed convolved action has been presented, and then the proof that variation of this quantity did indeed result in a true variational principle followed. Here we elect to go about things in a different manner, wherein instead we form a virtual action quantity δA by convolving the governing equations with corresponding energy conjugate variational quantities and summing. This results in the following:

$$\begin{aligned} \delta A = & \delta u * \left[m\ddot{u} + (\dot{J} - \beta\dot{\theta}) - \dot{\bar{j}} \right] + \delta J * \left[\frac{1}{k} \ddot{J} - \dot{u} \right] \\ & + \delta \theta * \left[\frac{mc_\varepsilon}{T_o} \ddot{\theta} - \frac{1}{T_o} \dot{H}_i + \beta \dot{u}_k - \frac{1}{T_o} \dot{\bar{\Psi}} \right] + \delta H * \left[\frac{1}{hAT_o} \dot{H} + \frac{1}{T_o} \dot{\theta} \right] \end{aligned} \quad (5)$$

where the * indicates a temporal convolution. At this point we perform temporal integration-by-parts operations on all terms with the goal of having symmetry of the time derivatives on the virtual and real quantities. For some quantities this requires fractional integration-by-parts. The breve then represents a left half order temporal derivative. As a result, (5) can be rewritten as:

$$\begin{aligned} \delta A = & \left[\delta \dot{u} * m\dot{u} + \delta \dot{J} * \frac{1}{k} \dot{J} \right] + \left[\delta \dot{\theta} * \frac{mc_\varepsilon}{T_o} \dot{\theta} + \delta \dot{H} * \frac{1}{hAT_o} \dot{H} \right] \\ & + \left[\delta \ddot{u} * \ddot{J} - \delta \ddot{J} * \ddot{u} \right] + \left[\delta \ddot{\theta} * \beta \ddot{u} - \delta \ddot{u} * \beta \ddot{\theta} \right] + \left[\delta \ddot{H} * \frac{1}{T_o} \ddot{\theta} - \delta \ddot{\theta} * \frac{1}{T_o} \ddot{H} \right] \\ & - \left[\delta \ddot{u} * \ddot{\bar{j}} \right] - \left[\delta \ddot{\theta} * \frac{1}{T_o} \ddot{\bar{\Psi}} \right] \\ & + \delta u(t) \left[-m\dot{u}(0) - J(0) + \beta\theta(0) + \bar{j}(0) \right] + \delta J(t) \left[-\frac{1}{k} \dot{J}(0) + u(0) \right] \\ & + \delta \theta(t) \left[-\frac{mc_\varepsilon}{T_o} \dot{\theta}(0) + \frac{1}{T_o} H(0) - \beta u(0) + \frac{1}{T_o} \bar{\Psi}(0) \right] + \delta H(t) \left[-\frac{1}{hAT_o} H(0) - \frac{1}{T_o} \theta(0) \right] \\ & + \delta u(0) m\dot{u}(t) + \delta J(0) \frac{1}{k} \dot{J}(t) + \delta \theta(0) \frac{mc_\varepsilon}{T_o} \dot{\theta}(t) \end{aligned} \quad (6)$$

Interestingly, we recognize that the bracketed quantities in the fourth and fifth lines of the above equations represent precisely the necessary initial conditions for this problem, despite making no mention of these to this point. Additionally, the final line represents the zero variation constraints on the initial values of u , J , and θ , which should be expected. At this point we take out the final three lines of (6) and consider what is left to be the variation of a mixed convolved action $I_{C_{TL}}$ corresponding to the lumped dynamic thermoelastic problem at hand. After taking the variational operator outside of all of the brackets we have

$$\delta I_{C_{TL}} = \delta \left\{ \begin{aligned} & \frac{1}{2} \left[\dot{u} * m \dot{u} + \dot{J} * \frac{1}{k} \dot{J} \right] + \frac{1}{2} \left[\dot{\theta} * \frac{mc_\epsilon}{T_o} \dot{\theta} + \ddot{H} * \frac{1}{hAT_o} \ddot{H} \right] \\ & + \frac{1}{2} \left[\ddot{u} * \ddot{J} - \ddot{J} * \ddot{u} \right] + \frac{1}{2} \left[\ddot{\theta} * \beta \ddot{u} - \ddot{u} * \beta \ddot{\theta} \right] + \frac{1}{2} \left[\ddot{H} * \frac{1}{T_o} \ddot{\theta} - \ddot{\theta} * \frac{1}{T_o} \ddot{H} \right] \\ & - \left[\ddot{u} * \ddot{j} \right] - \left[\ddot{\theta} * \frac{1}{T_o} \ddot{\Psi} \right] \end{aligned} \right\} \quad (7)$$

Then for our final mixed convolved action corresponding to this problem we are left with

$$I_{C_{TL}} = \frac{1}{2} \left[\dot{u} * m \dot{u} + \dot{J} * \frac{1}{k} \dot{J} \right] + \frac{1}{2} \left[\dot{\theta} * \frac{mc_\epsilon}{T_o} \dot{\theta} + \ddot{H} * \frac{1}{hAT_o} \ddot{H} \right] \\ + \frac{1}{2} \left[\ddot{u} * \ddot{J} - \ddot{J} * \ddot{u} \right] + \frac{1}{2} \left[\ddot{\theta} * \beta \ddot{u} - \ddot{u} * \beta \ddot{\theta} \right] + \frac{1}{2} \left[\ddot{H} * \frac{1}{T_o} \ddot{\theta} - \ddot{\theta} * \frac{1}{T_o} \ddot{H} \right] \\ - \left[\ddot{u} * \ddot{j} \right] - \left[\ddot{\theta} * \frac{1}{T_o} \ddot{\Psi} \right] \quad (8)$$

If one was to now reverse the order of this process by beginning with the mixed convolved action $I_{C_{TL}}$, then extremize by setting the first variation to zero, and perform temporal integration-by-parts operations on all terms, they would be left with Euler-Lagrange equations corresponding to the four governing equations (4a-d), the following correct initial conditions for the problem at hand:

$$m\dot{u}(0) + J(0) - \beta\theta(0) = \ddot{j}(0) \quad (9a)$$

$$\frac{1}{k} \dot{J}(0) - u(0) = 0 \quad (9b)$$

$$\frac{mc_\epsilon}{T_o} \dot{\theta}(0) + \beta u(0) - \frac{1}{T_o} H(0) = \frac{1}{T_o} \bar{\Psi}(0) \quad (9c)$$

$$\frac{1}{hAT_o} H(0) + \frac{1}{T_o} \theta(0) = 0 \quad (9d)$$

and variation constraints at time equals zero:

$$\delta u(0) = \delta \theta(0) = \delta J(0) = 0 \quad (10)$$

Thus, a *Principle of Stationary Mixed Convolved Action for Lumped Linear Thermoelasticity* has been developed. This may be stated as follows: Of all the possible trajectories $\{u(\tau), J(\tau), \theta(\tau), H(\tau)\}$ of the system during the time interval $(0, t)$, the one that renders the action $I_{C_{TL}}$ in (8) stationary, corresponds to the solution of the initial value problem. This stationary trajectory satisfies the balance laws of linear momentum (4a) and energy (4c), along with the linear elastic compatibility equation (4b) and Newton's law of cooling (4d) over the entire time interval. Additionally, the solution complies with all appropriate initial conditions and constraints on variations defined by (9)-(10).

Notably, the approach taken here presents a straight forward way to derive mixed convolved actions for a great variety of initial value problems, perhaps most importantly problems involving dissipation, for which previously true variational principles have been non-existent. Also interestingly, following the procedures here, where one begins with the governing differential equations, written in terms of mixed impulsive variables, convolves with proper virtual quantities, and then performs integration-by-parts operations, actually produces all appropriate initial conditions without any necessary prior knowledge of these conditions.

3. Fundamental continuum relations

In this section, we provide the foundation for the development of a pure variational statement for the continuum problem of dynamic coupled thermoelasticity, which represents the first formulation of this kind for multi-physical phenomena. Here, heat conduction is a dissipative process, coupled to the otherwise conservative elastic stress field. We also include second sound effects throughout the entirety of this work. In a way, this formalism can be regarded as the evolution of previous work on the thermoelastic problem by Apostolakis and Dargush (2012, 2013), which used instead an inner product action variation based upon Lagrangian energy and Rayleigh dissipation functionals, and the separate mixed convolved action variational statements for elastodynamics and heat conduction (Dargush et al., 2015, 2016).

For our mixed formulation of this problem, let the elastic response be represented by the displacement u_i and the impulse of the elastic stresses J_{ij} (Sivaselvan and Reinhorn, 2006). For consistency, one can view displacement u_i as the impulse of the velocity v_i . Meanwhile, as in Apostolakis and Dargush (2012, 2013), the thermal field will be described by θ , which represents the impulse of the temperature T and the heat vector H_i . For consistency, the heat vector H_i can be considered as the impulse of the heat flux q_i . Thus, for continuum thermoelasticity, we may write these variables in integral form as

$$u_i(t) = \int_0^t v_i(t) dt \quad (11a)$$

$$J_{ij}(t) = \int_0^t (\sigma_{ij}(t) + \beta_{ij} T(t)) dt = \int_0^t \sigma_{ij}^e(t) dt = \int_0^t C_{ijkl} \varepsilon_{kl}(t) dt \quad (11b)$$

$$\theta(t) = \int_0^t T(t) dt \quad (11c)$$

$$H_i(t) = \int_0^t q_i(t) dt \quad (11d)$$

with the corresponding rate form:

$$\dot{u}_i = v_i \quad (12a)$$

$$\dot{J}_{ij} = (\sigma_{ij} + \beta_{ij}T) = \sigma_{ij}^e = C_{ijkl}\varepsilon_{kl} \quad (12b)$$

$$\dot{\theta} = T \quad (12c)$$

$$\dot{H}_i = q_i \quad (12d)$$

where σ_{ij} and ε_{ij} represent the total stress and strain tensors, while C_{ijkl} and β_{ij} are the usual constitutive tensors for anisotropic thermoelastic media. Additionally, in (11b) and (12b), σ_{ij}^e are the purely elastic stresses associated with the total strains. By selecting the primary variables in this manner, we shall find that a more complete symmetry is obtained in the governing equations of thermoelasticity.

In terms of these mixed variables, the governing differential equations for coupled dynamic thermoelastic response, including second sound effects based upon the Lord and Shulman (1967) formulation, take the following form over the domain Ω :

$$\rho_o \ddot{u}_k - B_{ijk} (\dot{J}_{ij} - \beta_{ij} \dot{\theta}) = \bar{f}_k \quad (13a)$$

$$-A_{ijkl} \ddot{J}_{kl} + B_{ijk} \dot{u}_k = 0 \quad (13b)$$

$$\frac{\rho_o c_\varepsilon}{T_o} \ddot{\theta} + \frac{1}{T_o} B_i \dot{H}_i + \beta_{ij} B_{ijk} \dot{u}_k = \frac{1}{T_o} \bar{\psi} \quad (13c)$$

$$-d_{ij} \tau_o \frac{1}{T_o} \ddot{H}_j - d_{ij} \frac{1}{T_o} \dot{H}_j - \frac{1}{T_o} B_i \dot{\theta} = 0 \quad (13d)$$

In the above governing equations, ρ_o is the mass density, A_{ijkl} is the elastic constitutive tensor inverse to C_{ijkl} and \bar{f}_k is the specified body force density. For the thermal aspects of this problem, T_o represents the initial temperature at the free stress state, while T then becomes the temperature change from that state. Additionally, c_ε is the specific heat at constant strain, τ_o is a relaxation time for the extended Fourier's heat conduction law and $\bar{\psi}$ is a specified heat source density. The constitutive tensor d_{ij} represents the inverse of the thermal conductivity k_{ij} and the thermoelastic coupling tensor becomes $\beta_{ij} = 3\alpha\kappa \delta_{ij}$ for

the isotropic materials considered later, where α is the thermal expansion coefficient and κ is the bulk modulus. The symbol B_i in (13c,d) represents the gradient operator, while B_{ijk} is a third order tensor operator that extracts strain rates from the velocity field. Thus, we have

$$\dot{\epsilon}_{ij} = B_{ijk} \dot{u}_k \quad (14)$$

where more specifically

$$B_{ijk} = \frac{1}{2} (\delta_{ik} \delta_{jq} + \delta_{iq} \delta_{jk}) \frac{\partial}{\partial x_q} \quad (15)$$

with x_q representing spatial coordinates. The relation (14) may also be written in the more familiar manner as

$$\dot{\epsilon}_{ij} = \frac{1}{2} (\dot{u}_{i,j} + \dot{u}_{j,i}) \quad (16)$$

with the comma now symbolizing differentiation with respect to the spatial coordinates.

In addition to the governing differential equations, boundary conditions must be specified. For the simplest form, these can be written:

$$u_k = \bar{u}_k \quad \text{on } \Gamma_v \quad (17a)$$

$$\dot{J}_{jk} n_j - \beta_{jk} \dot{\theta} n_j = \sigma_{jk} n_j = \bar{t}_k \quad \text{on } \Gamma_t \quad (17b)$$

$$\theta = \bar{\theta} \quad \text{on } \Gamma_T \quad (17c)$$

$$\dot{H}_i n_i = \bar{q} \quad \text{on } \Gamma_q \quad (17d)$$

where \bar{u}_k and $\bar{\theta}$ represent essential boundary conditions of displacement and temperature impulse applied on the surfaces Γ_v and Γ_T , respectively. Meanwhile, for the natural boundary conditions, \bar{t}_k are the tractions specified on the portion of the surface Γ_t , while \bar{q} represents the specified normal heat flux on Γ_q .

Then, to complete the definition of the coupled dynamic thermoelasticity problem, initial conditions are required. In mixed variables, these take the following form at time zero:

$$\rho_o \dot{u}_k(0) - B_{ijk} (J_{ij}(0) - \beta_{ij} \theta(0)) = \bar{j}_k(0) \quad (18a)$$

$$-A_{ijkl} \dot{J}_{kl}(0) + B_{ijk} u_k(0) = 0 \quad (18b)$$

$$\frac{\rho_o c_\varepsilon}{T_o} \dot{\theta}(0) + \frac{1}{T_o} B_i H_i(0) + \beta_{ij} B_{ijk} u_k(0) = \frac{1}{T_o} \bar{\Psi}(0) \quad (18c)$$

$$-d_{ij} \tau_o \frac{1}{T_o} \dot{H}_j(0) - d_{ij} \frac{1}{T_o} H_j(0) - \frac{1}{T_o} B_i \theta(0) = 0 \quad (18d)$$

for $x \in \Omega$

where \bar{j}_k and $\bar{\Psi}$ are the impulses of \bar{f}_k and $\bar{\psi}$, respectively.

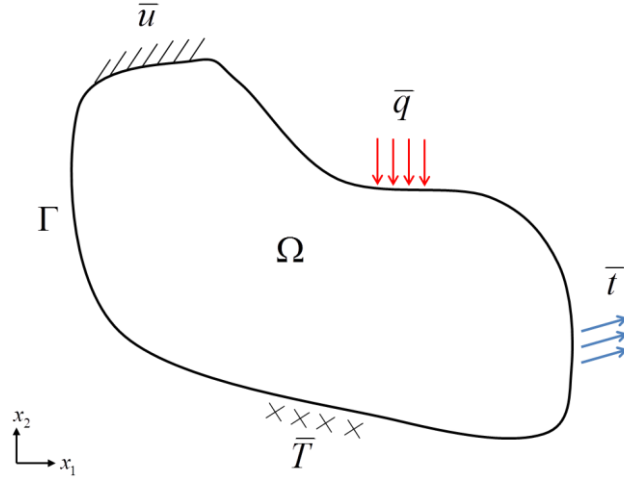


Fig. 2. Continuum thermoelasticity problem definition

4. Mixed convolved action for thermoelastic continua

In analogy with the elastodynamic and heat diffusion mixed convolved actions (Dargush et al., 2015, 2016), the inner product thermoelastic continuum formulation from Apostolakis and Dargush (2012, 2013), and the lumped thermoelastic system of Section 2, we may write the following scalar thermoelastic mixed convolved action functional:

$$\begin{aligned}
I_{C_T} = & \int_{\Omega} \left[\frac{1}{2} \dot{\tilde{u}}_k * \rho_o \dot{\tilde{u}}_k - \frac{1}{2} \dot{\tilde{J}}_{ij} * A_{ijkl} \dot{\tilde{J}}_{kl} \right] d\Omega \\
& - \int_{\Omega} \left[\frac{1}{2} \dot{\tilde{\theta}} * \frac{\rho_o C_c}{T_o} \dot{\tilde{\theta}} - \frac{1}{2} \dot{\tilde{H}}_i * d_{ij} \frac{\tau_o}{T_o} \dot{\tilde{H}}_j - \frac{1}{2} \tilde{H}_i * d_{ij} \frac{1}{T_o} \tilde{H}_j \right] d\Omega \\
& + \int_{\Omega} \left[\frac{1}{2} (\tilde{J}_{ij} * B_{ijk} \tilde{u}_k - \tilde{u}_k * B_{ijk} \tilde{J}_{ij}) \right] d\Omega \\
& - \int_{\Omega} \left[\frac{1}{2} (\beta_{ij} \tilde{\theta} * B_{ijk} \tilde{u}_k - \tilde{u}_k * B_{ijk} \beta_{ij} \tilde{\theta}) \right] d\Omega \\
& + \int_{\Omega} \left[\frac{1}{2} \left(\tilde{H}_i * \frac{1}{T_o} B_i \tilde{\theta} - \tilde{\theta} * \frac{1}{T_o} B_i \tilde{H}_i \right) \right] d\Omega \\
& - \int_{\Omega} \left[\tilde{u}_k * \tilde{j}_k \right] d\Omega + \int_{\Omega} \left[\tilde{\theta} * \frac{1}{T_o} \tilde{\Psi} \right] d\Omega \\
& - \int_{\Gamma_t} \frac{1}{2} \left[\tilde{u}_k * \tilde{\tau}_k \right] d\Gamma + \int_{\Gamma_v} \frac{1}{2} \left[\tilde{\tau}_k * \tilde{u}_k \right] d\Gamma \\
& - \int_{\Gamma_q} \frac{1}{2} \left[\tilde{\theta} * \frac{1}{T_o} \tilde{Q} \right] d\Gamma + \int_{\Gamma_r} \frac{1}{2} \left[\frac{1}{T_o} \tilde{Q} * \tilde{\theta} \right] d\Gamma
\end{aligned} \tag{19}$$

In (19) we again use a superposed dot and breve to represent integer and left half-order temporal derivatives, respectively, along with the * symbol to indicate a temporal convolution. Additionally, we use an overbar to denote quantities not subject to variation. In particular, in (19), $\overline{\tilde{j}}_k$ represents the impulse of the applied body force density $\overline{\tilde{f}}_k$, while $\overline{\tilde{\tau}}_k$ is the impulse $\overline{\tilde{t}}_k$, the applied surface tractions on a portion of the surface designated as Γ_t . In a similar way, $\overline{\tilde{u}}_k$ represents the enforced surface displacements on Γ_v , with τ_k as the impulse of the resulting reactive tractions t_k on that surface. Here, we assume that the boundary conditions are defined, such that $\Gamma_v \cup \Gamma_t = \Gamma$ and $\Gamma_v \cap \Gamma_t = \emptyset$. Furthermore, $\overline{\tilde{Q}}$ denotes the impulse

of \bar{q} , which represents the specified normal heat fluxes on the surface Γ_q . On Γ_T ,

$$Q(t) = H_i(t)n_i = \int_0^t q_i(t)n_i dt \text{ with } n_i \text{ as the outer unit normal to the surface.}$$

Then, the first variation of the mixed convolved action becomes

$$\begin{aligned} \delta I_{C_T} = & \int_{\Omega} \left[\delta \dot{u}_k * \rho_o \dot{u}_k - \delta \dot{J}_{ij} * A_{ijkl} \dot{J}_{kl} \right] d\Omega \\ & - \int_{\Omega} \left[\delta \dot{\theta} * \frac{\rho_o c_e}{T_o} \dot{\theta} - \delta \dot{H}_i * d_{ij} \frac{\tau_o}{T_o} \dot{H}_j - \delta \ddot{H}_i * d_{ij} \frac{1}{T_o} \ddot{H}_j \right] d\Omega \\ & + \int_{\Omega} \left[\frac{1}{2} \left(\delta \ddot{J}_{ij} * B_{ijk} \ddot{u}_k - \delta \ddot{u}_k * B_{ijk} \ddot{J}_{ij} + B_{ijk} \delta \ddot{u}_k * \ddot{J}_{ij} - B_{ijk} \delta \ddot{J}_{ij} * \ddot{u}_k \right) \right] d\Omega \\ & - \int_{\Omega} \left[\frac{1}{2} \left(\beta_{ij} \delta \ddot{\theta} * B_{ijk} \ddot{u}_k - \delta \ddot{u}_k * B_{ijk} \beta_{ij} \ddot{\theta} + B_{ijk} \delta \ddot{u}_k * \beta_{ij} \ddot{\theta} - B_{ijk} \beta_{ij} \delta \ddot{\theta} * \ddot{u}_k \right) \right] d\Omega \\ & + \int_{\Omega} \left[\frac{1}{2} \left(\delta \ddot{H}_i * \frac{1}{T_o} B_i \ddot{\theta} - \delta \ddot{\theta} * \frac{1}{T_o} B_i \ddot{H}_i + \frac{1}{T_o} B_i \delta \ddot{\theta} * \ddot{H}_i - \frac{1}{T_o} B_i \delta \ddot{H}_i * \ddot{\theta} \right) \right] d\Omega \\ & - \int_{\Omega} \left[\delta \ddot{u}_k * \ddot{j}_k \right] d\Omega + \int_{\Omega} \left[\delta \ddot{\theta} * \frac{1}{T_o} \ddot{\Psi} \right] d\Omega \\ & - \int_{\Gamma_i} \frac{1}{2} \left[\delta \ddot{u}_k * \ddot{\tau} \right] d\Gamma + \int_{\Gamma_v} \frac{1}{2} \left[\delta \ddot{\tau}_k * \ddot{u}_k \right] d\Gamma \\ & - \int_{\Gamma_q} \frac{1}{2} \left[\delta \ddot{\theta} * \frac{1}{T_o} \ddot{Q} \right] d\Gamma + \int_{\Gamma_T} \frac{1}{2} \left[\frac{1}{T_o} \delta \ddot{Q} * \ddot{\theta} \right] d\Gamma \end{aligned} \quad (20)$$

After performing all of the temporal classical and fractional integration-by-parts operations (Dargush and Kim, 2012) to shift derivatives from the variations to the field variables, the stationarity of the mixed convolved action may be written in the following complicated, but systematic form:

$$\begin{aligned}
\delta I_{C_r} = & \int_{\Omega} \delta u_k * [\rho_o \ddot{u}_k - B_{ijk} (\dot{J}_{ij} - \beta_{ij} \dot{\theta}) - \bar{f}_k] d\Omega + \int_{\Omega} \delta J_{ij} * [-A_{ijkl} \ddot{J}_{kl} + B_{ijk} \dot{u}_k] d\Omega \\
& - \int_{\Omega} \delta \theta * \left[\frac{\rho_o c_\varepsilon}{T_o} \ddot{\theta} + \frac{1}{T_o} B_i \dot{H}_i + \beta_{ij} B_{ijk} \dot{u}_k - \frac{1}{T_o} \bar{\psi} \right] d\Omega \\
& - \int_{\Omega} \delta H_i * \left[-d_{ij} \tau_o \frac{1}{T_o} \ddot{H}_j - d_{ij} \frac{1}{T_o} \dot{H}_j - \frac{1}{T_o} B_i \dot{\theta} \right] d\Omega \\
& + \int_{\Omega} \delta u_k(t) [\rho_o \dot{u}_k(0) - B_{ijk} (J_{ij}(0) - \beta_{ij} \theta(0)) - \bar{J}_k(0)] d\Omega - \int_{\Omega} \delta u_k(0) [\rho_o \dot{u}_k(t)] d\Omega \\
& + \int_{\Omega} \delta J_{ij}(t) [-A_{ijkl} \dot{J}_{kl}(0) + B_{ijk} u_k(0)] d\Omega - \int_{\Omega} \delta J_{ij}(0) [-A_{ijkl} \dot{J}_{kl}(t)] d\Omega \\
& - \int_{\Omega} \delta \theta(t) \left[\frac{\rho_o c_\varepsilon}{T_o} \dot{\theta}(0) + \frac{1}{T_o} B_i H_i(0) + \beta_{ij} B_{ijk} u_k(0) - \frac{1}{T_o} \bar{\Psi}(0) \right] d\Omega \\
& - \int_{\Omega} \delta \theta(0) \left[\frac{\rho_o c_\varepsilon}{T_o} \dot{\theta}(t) \right] d\Omega \\
& - \int_{\Omega} \delta H_i(t) \left[-d_{ij} \tau_o \frac{1}{T_o} \dot{H}_j(0) - d_{ij} \frac{1}{T_o} H_j(0) - \frac{1}{T_o} B_i \theta(0) \right] d\Omega \\
& - \int_{\Omega} \delta H_i(0) \left[-d_{ij} \tau_o \frac{1}{T_o} \dot{H}_j(t) \right] d\Omega \\
& + \int_{\Gamma_r} \frac{1}{2} [\delta u_k * t_k - \delta u_k * \bar{t}_k] d\Gamma + \int_{\Gamma_r} \frac{1}{2} [\delta u_k(t) \tau_k(0) - \delta u_k(t) \bar{\tau}_k(0)] d\Gamma \\
& + \int_{\Gamma_v} \frac{1}{2} [\delta u_k * t_k] d\Gamma + \int_{\Gamma_v} \frac{1}{2} [\delta u_k(t) \tau_k(0)] d\Gamma \\
& - \int_{\Gamma_v} \frac{1}{2} [\delta \tau_k * v_k - \delta \tau_k * \bar{v}_k] d\Gamma - \int_{\Gamma_v} \frac{1}{2} [\delta \tau_k(t) u_k(0) - \delta \tau_k(t) \bar{u}_k(0)] d\Gamma \\
& - \int_{\Gamma_v} \frac{1}{2} [\delta \tau_k * v_k] d\Gamma - \int_{\Gamma_v} \frac{1}{2} [\delta \tau_k(t) u_k(0)] d\Gamma \\
& + \int_{\Gamma_q} \frac{1}{2T_o} [\delta \theta * q - \delta \theta * \bar{q}] d\Gamma + \int_{\Gamma_q} \frac{1}{2T_o} [\delta \theta(t) Q(0) - \delta \theta(t) \bar{Q}(0)] d\Gamma \\
& + \int_{\Gamma_r} \frac{1}{2T_o} [\delta \theta * q] d\Gamma + \int_{\Gamma_r} \frac{1}{2T_o} [\delta \theta(t) Q(0)] d\Gamma \\
& - \int_{\Gamma_r} \frac{1}{2T_o} [\delta Q * T - \delta Q * \bar{T}] d\Gamma - \int_{\Gamma_r} \frac{1}{2T_o} [\delta Q(t) \theta(0) - \delta Q(t) \bar{\theta}(0)] d\Gamma \\
& - \int_{\Gamma_q} \frac{1}{2T_o} [\delta Q * T] d\Gamma - \int_{\Gamma_q} \frac{1}{2T_o} [\delta Q(t) \theta(0)] d\Gamma = 0
\end{aligned} \tag{21}$$

From (21) for arbitrary variations, we have as the Euler-Lagrange equations:

Governing partial differential equations

$$\rho_o \ddot{u}_k - B_{ijk} (\dot{J}_{ij} - \beta_{ij} \dot{\theta}) = \bar{f}_k \tag{22a}$$

$$-A_{ijkl} \ddot{J}_{kl} + B_{ijk} \dot{u}_k = 0 \tag{22b}$$

$$\frac{\rho_o c_\varepsilon}{T_o} \ddot{\theta} + \frac{1}{T_o} B_i \dot{H}_i + \beta_{ij} B_{ijk} \dot{u}_k = \frac{1}{T_o} \bar{\psi} \quad (22c)$$

$$-d_{ij} \tau_o \frac{1}{T_o} \ddot{H}_j - d_{ij} \frac{1}{T_o} \dot{H}_j - \frac{1}{T_o} B_i \dot{\theta} = 0 \quad (22d)$$

for $x \in \Omega$, $\tau \in (0, t)$

Boundary conditions over the entire time span

$$t_k = \bar{t}_k \quad x \in \Gamma_t \quad (23a)$$

$$v_k = \bar{v}_k \quad x \in \Gamma_v \quad (23b)$$

$$q = \bar{q} \quad x \in \Gamma_q \quad (23c)$$

$$T = \bar{T} \quad x \in \Gamma_T \quad (23d)$$

for $\tau \in (0, t)$

Initial conditions over the spatial domain

$$\rho_o \dot{u}_k(0) - B_{ijk} (J_{ij}(0) - \beta_{ij} \theta(0)) = \bar{j}_k(0) \quad (24a)$$

$$-A_{ijkl} \dot{J}_{kl}(0) + B_{ijk} u_k(0) = 0 \quad (24b)$$

$$\frac{\rho_o c_\varepsilon}{T_o} \dot{\theta}(0) + \frac{1}{T_o} B_i H_i(0) + \beta_{ij} B_{ijk} u_k(0) = \frac{1}{T_o} \bar{\Psi}(0) \quad (24c)$$

$$-d_{ij} \tau_o \frac{1}{T_o} \dot{H}_j(0) - d_{ij} \frac{1}{T_o} H_j(0) - \frac{1}{T_o} B_i \theta(0) = 0 \quad (24d)$$

for $x \in \Omega$

Boundary conditions at time zero

$$\tau_k(0) = \bar{\tau}_k(0) \quad x \in \Gamma_t \quad (25a)$$

$$u_k(0) = \bar{u}_k(0) \quad x \in \Gamma_v \quad (25b)$$

$$Q(0) = \bar{Q}(0) \quad x \in \Gamma_q \quad (25c)$$

$$\theta(0) = \bar{\theta}(0) \quad x \in \Gamma_T \quad (25d)$$

Furthermore, the variations are defined with the following constraints:

Zero variations for specified boundary conditions

$$\delta\tau_k = 0 \quad x \in \Gamma_t, \tau \in (0, t) \quad (26a)$$

$$\delta u_k = 0 \quad x \in \Gamma_v, \tau \in (0, t) \quad (26b)$$

$$\delta Q = 0 \quad x \in \Gamma_q, \tau \in (0, t) \quad (26c)$$

$$\delta\theta = 0 \quad x \in \Gamma_T, \tau \in (0, t) \quad (26d)$$

Zero variations at initial time

$$\delta u_k(0) = 0 \quad x \in \Omega \quad (27a)$$

$$\delta J_{ij}(0) = 0 \quad x \in \Omega \quad (27b)$$

$$\delta\theta(0) = 0 \quad x \in \Omega \quad (27c)$$

$$\delta H_i(0) = 0 \quad x \in \Omega \quad (27d)$$

Zero end time variations for specified boundary conditions

$$\delta\tau_k(t) = 0 \quad x \in \Gamma_t \quad (28a)$$

$$\delta u_k(t) = 0 \quad x \in \Gamma_v \quad (28b)$$

$$\delta Q(t) = 0 \quad x \in \Gamma_q \quad (28c)$$

$$\delta\theta(t) = 0 \quad x \in \Gamma_T \quad (28d)$$

Consequently, we have now established a *Principle of Stationary Mixed Convolved Action for a Linear Thermoelastic Continuum* undergoing infinitesimal deformation. This may be stated as follows: Of all the possible trajectories $\{u_k(\tau), J_{ij}(\tau), \theta(\tau), H_i(\tau)\}$ of the system during the time interval $(0, t)$, the one that renders the action I_{C_T} in (19) stationary, corresponds to the solution of the initial/boundary value problem.

Thus, the stationary trajectory satisfies the balance laws of linear momentum (22a) and energy (22c), along

with the linear thermoelastic constitutive relationship (22b) and the extended Fourier law of heat conduction (22d) in the domain Ω over the entire time interval. In addition, the traction (23a), velocity (23b), heat flux (23c) and temperature (23d) boundary conditions are satisfied throughout the time interval, while also complying with the initial conditions defined by (24a-d) in Ω and (25a-d) on the appropriate portions of the bounding surface. Furthermore, the possible trajectories under consideration during the variational process are constrained precisely by their need to satisfy the specified initial and boundary conditions of the problem in the form of (26a-d), (27a-d) and (28a-d).

Remarkably, we are able to define a single real scalar functional I_{C_r} , based upon convolution and fractional derivatives, which encapsulates all of the governing differential equations, along with the boundary and initial conditions, for dynamic thermoelasticity. This represents the first true mixed variational formulation for a dissipative thermomechanical continuum and demonstrates the ability of the mixed convolved action approach to address multi-physics phenomena.

5. Finite element formulations in space and time

In this section we will develop a computational framework using finite elements for both space and time, but first we need to define a suitable weak form. While the first variation of the MCA represented by equation (20) could be used as the weak form, it is not unique, as any number of integration by parts operations can be applied to it, resulting in a new weak form. Here we choose to modify the continuity requirements associated with equation (20) by moving all spatial derivatives onto the displacements u_i and the temperature impulses θ . Then, starting with equation (20) and performing spatial integration by parts on the terms involving first order spatial derivatives of stress impulse J_{ij} and the heat vector H_i yields the following expression:

$$\begin{aligned}
\delta I_{C_{TE}} = & \int_{\Omega} \left[\delta \dot{u}_k * \rho_o \dot{u}_k - \delta \dot{J}_{ij} * A_{ijkl} \dot{J}_{kl} \right] d\Omega \\
& + \int_{\Omega} \left[\delta \ddot{J}_{ij} * B_{ijk} \ddot{u}_k + B_{ijk} \delta \ddot{u}_k * \ddot{J}_{ij} \right] d\Omega \\
& - \int_{\Omega} \left[\delta \dot{\theta} * \frac{\rho_o c_c}{T_o} \dot{\theta} - \delta \dot{H}_i * d_{ij} \frac{\tau_o}{T_o} \dot{H}_j - \delta \ddot{H}_i * d_{ij} \frac{1}{T_o} \ddot{H}_j \right] d\Omega \\
& + \int_{\Omega} \left[\delta \ddot{H}_i * \frac{1}{T_o} B_i \ddot{\theta} + \frac{1}{T_o} B_i \delta \ddot{\theta} * \ddot{H}_i \right] d\Omega \\
& - \int_{\Omega} \left[\delta \ddot{\theta} * \beta_{ij} B_{ijk} \ddot{u}_k + \beta_{ij} B_{ijk} \delta \ddot{u}_k * \ddot{\theta} \right] \\
& - \int_{\Omega} \left[\delta \ddot{u}_k * \ddot{J}_k \right] d\Omega + \int_{\Omega} \left[\delta \ddot{\theta} * \frac{1}{T_o} \ddot{\Psi} \right] d\Omega \\
& - \int_{\Gamma_r} \frac{1}{2} \left[\delta \ddot{u}_k * (\ddot{\tau}_k + \ddot{\tau}_k) \right] d\Gamma + \int_{\Gamma_v} \frac{1}{2} \left[\delta \ddot{\tau}_k * (\ddot{u}_k - \ddot{u}_k) \right] d\Gamma \\
& - \int_{\Gamma_q} \frac{1}{2T_o} \left[\delta \ddot{\theta} * (\ddot{Q} + \ddot{Q}) \right] d\Gamma + \int_{\Gamma_T} \frac{1}{2T_o} \left[\delta \ddot{Q} * (\ddot{\theta} - \ddot{\theta}) \right] d\Gamma \\
= & 0
\end{aligned} \tag{29}$$

Equation (29) is now the weak form on which we will base our numerical methodology.

We proceed with the development of a finite element formulation based on (29). In the present work, we will only deal with two-dimensional problems, however most of the equations either generally apply to three-dimensional problems also, or can be simply extended for full three-dimensional analysis. The weak form selected above was of course not arbitrary but chosen because of the location of the spatial derivative B operators. In (29), we have only first order spatial derivatives of displacements, temperature impulses, and the variations of these field variables. Then for a convergent formulation we must enforce at least C^0 continuity in space for these quantities, while for impulse of stress and heat flux fields only C^{-1} continuity need be enforced. This means that for the simplest case we can use linear spatial interpolation for displacements and temperature impulses, while we can consider the other quantities to be constant throughout the element and generally discontinuous across element boundaries. Temporally, first order derivatives appear for each field variable, so we must maintain C^0 continuity in time, which for the simplest

finite element scheme refers to using linear shape functions in time. We should emphasize that while the impulses of stress and heat flux must be continuous in time due to the appearance of first order derivatives in (29), generally, the stresses and heat fluxes need not be.

It is important to again note the absence of the end time constraints that appear in any application of Hamilton's principle. This allows for very natural use of temporal finite elements for the discretized version of (29) without needing to resort to some of the ad-hoc methods of dealing with this constraint that other variational approaches have required (Kane et al., 1999, 2000; Marsden and West, 2001; Sivaselvan and Reinhorn, 2006; Sivaselvan et. al., 2009; Apostolakis and Dargush, 2012, 2013).

Upon spatial discretization of our domain and spatial integration we can then write the terms appearing in the weak form of (29) as

$$\int_{\Omega_e} \delta \dot{u}_k * \rho_o \dot{u}_k d\Omega = \delta \dot{\mathbf{u}}^T * \mathbf{M}_{uu} \dot{\mathbf{u}} \quad (30a)$$

$$\int_{\Omega_e} \delta \dot{J}_{ij} * A_{ijkl} \dot{J}_{kl} d\Omega = \delta \dot{\mathbf{J}}^T * \mathbf{A}_{JJ} \dot{\mathbf{J}} \quad (30b)$$

$$\int_{\Omega_e} \delta \tilde{J}_{ij} * B_{ijk} \tilde{u}_k d\Omega = \delta \tilde{\mathbf{J}}^T * \mathbf{B}_{Ju} \tilde{\mathbf{u}} \quad (30c)$$

$$\int_{\Omega_e} B_{ijk} \delta \tilde{u}_k * \tilde{J}_{ij} d\Omega = \delta \tilde{\mathbf{u}}^T \mathbf{B}_{Ju}^T * \tilde{\mathbf{J}} \quad (30d)$$

$$\int_{\Omega_e} \delta \dot{\theta} * \frac{\rho_o c_\epsilon}{T_o} \dot{\theta} d\Omega = \delta \dot{\boldsymbol{\theta}}^T * \mathbf{M}_{\theta\theta} \dot{\boldsymbol{\theta}} \quad (31a)$$

$$\int_{\Omega_e} \delta \dot{H}_i * d_{ij} \frac{\tau_o}{T_o} \dot{H}_j d\Omega = \delta \dot{\mathbf{H}}^T * \mathbf{A}_{HH} \dot{\mathbf{H}} \quad (31b)$$

$$\int_{\Omega_e} \delta \tilde{H}_i * d_{ij} \frac{1}{T_o} \tilde{H}_j d\Omega = \delta \tilde{\mathbf{H}}^T * \mathbf{D}_{HH} \tilde{\mathbf{H}} \quad (31c)$$

$$\int_{\Omega_e} \delta \tilde{H}_i * \frac{1}{T_o} B_i \tilde{\theta} d\Omega = \delta \tilde{\mathbf{H}}^T * \mathbf{B}_{H\theta} \tilde{\boldsymbol{\theta}} \quad (31d)$$

$$\int_{\Omega_e} \frac{1}{T_o} B_i \delta \tilde{\theta} * \tilde{H}_i d\Omega = \delta \tilde{\theta}^T \mathbf{B}_{H\theta}^T * \tilde{\mathbf{H}} \quad (31e)$$

$$\int_{\Omega_e} \delta \tilde{\theta} * \beta_{ij} B_{ijk} \tilde{u}_k d\Omega = \delta \tilde{\theta}^T * \mathbf{B}_{\theta u} \tilde{\mathbf{u}} \quad (32a)$$

$$\int_{\Omega_e} \beta_{ij} B_{ijk} \delta \tilde{u}_k * \tilde{\theta} d\Omega = \delta \tilde{\mathbf{u}}^T \mathbf{B}_{\theta u}^T * \tilde{\theta} \quad (32b)$$

where the bold face characters represent the discrete counterpart of a quantity. Here we wish to consider the simplest two-dimensional case, where we will use linear triangle elements for spatial interpolation of displacements and impulses of temperature. We then consider impulses of stress and heat flux to be constant throughout the element. The area shape functions can be written explicitly as

$$\mathbf{N}^T = \begin{pmatrix} 1 - \xi_1 - \xi_2 \\ \xi_1 \\ \xi_2 \end{pmatrix} \quad (33)$$

where ξ_i represent the local or natural element coordinates, which for the linear triangular elements are area coordinates. The shape functions, along with the Jacobian, are used to map our physical elements to the master isoparametric triangle element shown in Fig. 3, with coordinates ξ_1 and ξ_2 ranging from 0 to 1. Then we can represent the geometry of an element in terms of these local coordinates by interpolating the coordinates at nodes 1-3, such that

$$x = \mathbf{N} \mathbf{x} \quad (34a)$$

$$y = \mathbf{N} \mathbf{y} \quad (34b)$$

where now we use $x \equiv x_1$ and $y \equiv x_2$. The components of the Jacobian matrix for an element are then defined as

$$\mathbf{J}_{ij} \equiv \frac{\partial x_i}{\partial \xi_j} \quad (35)$$

such that

$$\mathbf{J} = \begin{pmatrix} \frac{\partial x}{\partial \xi_1} & \frac{\partial x}{\partial \xi_2} \\ \frac{\partial y}{\partial \xi_1} & \frac{\partial y}{\partial \xi_2} \end{pmatrix} \quad (36)$$

Then the area of an element, A , can be related to the determinant of the Jacobian by

$$A = |\mathbf{J}| / 2 \quad (37)$$

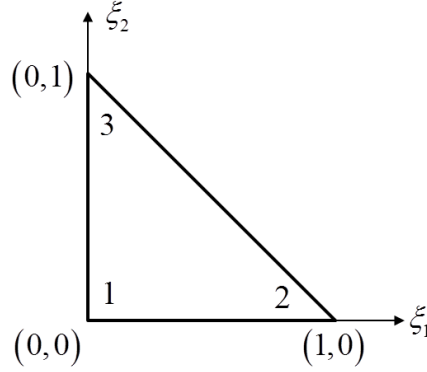


Fig. 3. Isoparametric master triangle element

Next we will define sub-matrices \mathbf{b}_i as

$$(\mathbf{b}_{Ju})_i = \begin{pmatrix} \frac{dN_i}{dx} & 0 \\ 0 & \frac{dN_i}{dy} \\ \frac{dN_i}{dy} & \frac{dN_i}{dx} \end{pmatrix} \quad (38a)$$

$$(\mathbf{b}_{H\theta})_i = \begin{pmatrix} \frac{dN_i}{dx} \\ \frac{dN_i}{dy} \end{pmatrix} \quad (38b)$$

$$(\mathbf{b}_{\theta u})_i = \begin{pmatrix} \frac{dN_i}{dx} & 0 \\ 0 & \frac{dN_i}{dy} \end{pmatrix} \quad (38c)$$

Then the full \mathbf{b} matrices can be written by concatenating the sub-matrices such that

$$\mathbf{b}_{Ju} = (\mathbf{b}_{Ju1} \quad \mathbf{b}_{Ju2} \quad \mathbf{b}_{Ju3}) \quad (39a)$$

$$\mathbf{b}_{H\theta} = (\mathbf{b}_{H\theta1} \quad \mathbf{b}_{H\theta2} \quad \mathbf{b}_{H\theta3}) \quad (39b)$$

$$\mathbf{b}_{\theta u} = (\mathbf{b}_{\theta u1} \quad \mathbf{b}_{\theta u2} \quad \mathbf{b}_{\theta u3}) \quad (39c)$$

and finally we can relate these \mathbf{b} matrices to the \mathbf{B} matrices appearing in our finite element formulation by

$$\mathbf{B}_{Ju} = \int_{\Omega_e} \mathbf{b}_{Ju} d\Omega \quad (40a)$$

$$\mathbf{B}_{H\theta} = \frac{1}{T_o} \int_{\Omega_e} \mathbf{b}_{H\theta} d\Omega \quad (40b)$$

$$\mathbf{B}_{\theta u} = \int_{\Omega_e} 3\alpha\kappa N^T \mathbf{b}_{\theta u} d\Omega \quad (40c)$$

where all integration is carried out numerically via Gauss quadrature. For more information on shape functions, mapped elements, and numerical integration the reader is referred to Bathe (1996) and Zienkiewicz and Taylor (2000).

The \mathbf{M} matrices are calculated as lumped mass matrices, such that we have

$$\mathbf{M}_{uu} = \rho_o A h \mathbf{I}_6 / 3 \quad (41a)$$

$$\mathbf{M}_{\theta\theta} = \frac{\rho_o c_c}{T_o} A h \mathbf{I}_3 / 3 \quad (41b)$$

while the other matrices are calculated as

$$\mathbf{A}_{JJ} = \frac{1+\nu}{E} A h \begin{bmatrix} 1-\nu & -\nu & 0 \\ -\nu & 1-\nu & 0 \\ 0 & 0 & 2 \end{bmatrix} \quad \text{for plane strain} \quad (42a)$$

$$\mathbf{A}_{JJ} = \frac{1}{E} A h \begin{bmatrix} 1 & -\nu & 0 \\ -\nu & 1 & 0 \\ 0 & 0 & 2(1+\nu) \end{bmatrix} \quad \text{for plane stress} \quad (42b)$$

$$\mathbf{A}_{HH} = \frac{\tau_o}{T_o k} A h \mathbf{I}_3 \quad (42c)$$

$$\mathbf{D}_{HH} = \frac{1}{T_o k} A h \mathbf{I}_3 \quad (42d)$$

where \mathbf{I}_n is a $[n \times n]$ identity matrix, α is the coefficient of thermal expansion, k is the thermal conductivity, ν is Poisson's ratio, and E is Young's modulus.

In a similar manner to the other terms appearing in the weak form (29), after spatial discretization, the body force contributions over an element become:

$$\int_{\Omega_e} \delta \tilde{u}_k * \tilde{j}_k d\Omega = \delta \tilde{\mathbf{u}}^T * \tilde{\mathbf{j}} \quad (43)$$

while the terms from the boundary conditions can be obtained by integration over an element edge, producing

$$\int_{\Gamma} \frac{1}{2} \left[\delta \tilde{u}_k * (\tilde{\tau}_k + \check{\tau}_k) \right] d\Gamma = \frac{1}{2} \delta \tilde{\mathbf{u}}^T * (\tilde{\boldsymbol{\tau}} + \check{\boldsymbol{\tau}}) \quad (44a)$$

$$\int_{\Gamma_v} \frac{1}{2} \left[\delta \check{\tau}_k * (\tilde{u}_k - \check{u}_k) \right] d\Gamma = \frac{1}{2} \delta \check{\boldsymbol{\tau}}^T * (\tilde{\mathbf{u}} - \check{\mathbf{u}}) \quad (44b)$$

where $\tilde{\mathbf{j}}$, $\tilde{\boldsymbol{\tau}}$, $\check{\boldsymbol{\tau}}$ and $\delta \check{\boldsymbol{\tau}}$ now include the contributions from the spatial integrations. Consistent with the appearance of overbars, the symbols $\tilde{\mathbf{u}}$ and $\check{\boldsymbol{\tau}}$ indicate known quantities that can be evaluated from the specified boundary conditions. Likewise, $\tilde{\mathbf{j}}$ is associated with known body force contributions. The corresponding terms in (44a,b) and (43) can then be included on the right hand side of the discrete form of the governing equations. On the other hand, the $\check{\mathbf{u}}$ and $\check{\boldsymbol{\tau}}$ appearing in (44a,b) are unknown surface variables, which can be related to nodal displacements and element stress impulses, respectively, and

therefore can contribute to the left hand side of the discretized representation. Because identical relations can be established for the variations $\delta\tilde{\mathbf{u}}$ and $\delta\tilde{\boldsymbol{\tau}}$, the ultimate contribution of these terms to the left hand side system matrix will be symmetric. However, an extrapolation of the element-based stress impulse variables \mathbf{J} may be required to form $\boldsymbol{\tau}$, unless these stress impulse variables include locations exactly on the element edges. In the present implementation, such is not the case. The \mathbf{J} variables are assumed constant within each element. This would provide only a very crude approximation of the unknown boundary traction impulses $\boldsymbol{\tau}$ and the resulting left half-order temporal derivatives $\tilde{\boldsymbol{\tau}}$. Consequently, here we simply equate the unknown variables to known values (i.e., $\tilde{\boldsymbol{\tau}} = \bar{\bar{\boldsymbol{\tau}}}$, $\tilde{\mathbf{u}} = \bar{\bar{\mathbf{u}}}$) on edges associated with Γ_t and Γ_v , such that the enforced tractions have a contribution defined by

$$\int_{\Gamma_t} \frac{1}{2} \left[\delta\tilde{\mathbf{u}}_k * (\bar{\bar{\boldsymbol{\tau}}}_k + \tilde{\boldsymbol{\tau}}_k) \right] d\Gamma = \delta\tilde{\mathbf{u}}^T * \bar{\bar{\boldsymbol{\tau}}} \quad (45a)$$

while the enforced displacement integral has no explicit additional effect, because

$$\int_{\Gamma_v} \frac{1}{2} \left[\delta\tilde{\boldsymbol{\tau}}_k * (\bar{\bar{\mathbf{u}}}_k - \tilde{\mathbf{u}}_k) \right] d\Gamma = 0 \quad (45b)$$

Similarly, for the heat terms, after spatial discretization, the body source contributions over an element can be written:

$$\int_{\Omega_e} \delta\tilde{\theta} * \frac{1}{T_o} \tilde{\Psi} d\Omega = \delta\tilde{\theta}^T * \tilde{\Psi} \quad (46)$$

while the terms from the boundary conditions can be evaluated through integration over an element edge, thus yielding

$$\int_{\Gamma_q} \frac{1}{2T_o} \left[\delta\tilde{\theta} * (\bar{\bar{\tilde{Q}}} + \tilde{\tilde{Q}}) \right] d\Gamma = \frac{1}{2} \delta\tilde{\theta}^T * (\bar{\bar{\tilde{Q}}} + \tilde{\tilde{Q}}) \quad (47a)$$

$$\int_{\Gamma_T} \frac{1}{2T_o} \left[\delta\tilde{\tilde{Q}} * (\bar{\bar{\tilde{\theta}}} - \tilde{\tilde{\theta}}) \right] d\Gamma = \frac{1}{2} \delta\tilde{\tilde{Q}}^T * (\bar{\bar{\tilde{\theta}}} - \tilde{\tilde{\theta}}) \quad (47b)$$

In a manner similar to our handling of the mechanical boundary condition terms, we simply equate the unknown variables to the known values (i.e., $\check{\mathbf{Q}} = \check{\check{\mathbf{Q}}}$, $\check{\boldsymbol{\theta}} = \check{\check{\boldsymbol{\theta}}}$) on edges associated with Γ_q and Γ_T , such that the enforced heat fluxes have a contribution defined by

$$\int_{\Gamma_q} \frac{1}{2T_o} \left[\delta\check{\boldsymbol{\theta}} * \left(\check{\check{\mathbf{Q}}} + \check{\mathbf{Q}} \right) \right] d\Gamma = \delta\check{\boldsymbol{\theta}}^T * \check{\check{\mathbf{Q}}} \quad (48a)$$

On the other hand, the enforced temperature impulse integral has no explicit additional effect, because

$$\int_{\Gamma_T} \frac{1}{2T_o} \left[\delta\check{\mathbf{Q}} * \left(\check{\check{\boldsymbol{\theta}}} - \check{\boldsymbol{\theta}} \right) \right] d\Gamma = 0 \quad (48b)$$

Note that for (46), (47) and (48) the factor of $1/T_o$ has been included, along with the effects of the volume and surface integrations, in the discretized terms on the right hand side to assure that all terms represent actions. Substituting the preceding discretized representations into equation (29) provides the spatially discretized mixed weak form for an element, which can be written:

$$\begin{aligned} & \delta\check{\mathbf{u}}^T * \mathbf{M}_{uu} \dot{\check{\mathbf{u}}} - \delta\check{\mathbf{J}}^T * \mathbf{A}_{JJ} \dot{\check{\mathbf{J}}} + \delta\check{\mathbf{J}}^T * \mathbf{B}_{Ju} \check{\mathbf{u}} + \delta\check{\mathbf{u}}^T \mathbf{B}_{Ju}^T * \check{\mathbf{J}} \\ & - \delta\check{\boldsymbol{\theta}}^T * \mathbf{M}_{\theta\theta} \dot{\check{\boldsymbol{\theta}}} + \delta\check{\mathbf{H}}^T * \mathbf{A}_{HH} \dot{\check{\mathbf{H}}} + \delta\check{\mathbf{H}}^T * \mathbf{D}_{HH} \check{\mathbf{H}} \\ & + \delta\check{\mathbf{H}}^T * \mathbf{B}_{H\theta} \check{\boldsymbol{\theta}} + \delta\check{\boldsymbol{\theta}}^T \mathbf{B}_{H\theta}^T * \check{\mathbf{H}} \\ & - \delta\check{\boldsymbol{\theta}}^T * \mathbf{B}_{\theta u} \check{\mathbf{u}} - \delta\check{\mathbf{u}}^T \mathbf{B}_{\theta u}^T * \check{\boldsymbol{\theta}} \\ & - \delta\check{\mathbf{u}}^T * \check{\check{\mathbf{j}}} - \delta\check{\mathbf{u}}^T * \check{\check{\boldsymbol{\tau}}} + \delta\check{\boldsymbol{\theta}}^T * \check{\check{\boldsymbol{\Psi}}} - \delta\check{\boldsymbol{\theta}}^T * \check{\check{\mathbf{Q}}} = 0 \end{aligned} \quad (49)$$

Next we must consider temporal discretization of the weak form. As previously mentioned, due to the presence of first derivatives, we must maintain at least C^0 continuity of our field variables versus time, thus linear shape functions are used for temporal interpolation. Then, over a time interval $0 \leq t \leq \Delta t$, we have:

$$\mathbf{u}(t) = \mathbf{u}_0 N_0(t) + \mathbf{u}_1 N_1(t) \quad (50a)$$

$$\mathbf{J}(t) = \mathbf{J}_0 N_0(t) + \mathbf{J}_1 N_1(t) \quad (50b)$$

$$\boldsymbol{\theta}(t) = \boldsymbol{\theta}_0 N_0(t) + \boldsymbol{\theta}_1 N_1(t) \quad (50c)$$

$$\mathbf{H}(t) = \mathbf{H}_0 N_0(t) + \mathbf{H}_1 N_1(t) \quad (50d)$$

in terms of the temporal shape functions

$$N_0(t) = 1 - \frac{t}{\Delta t}; \quad N_1(t) = \frac{t}{\Delta t} \quad (51a,b)$$

with similar temporal interpolation for the variations of our field variables, as well as applied force, traction, heat source, and flux terms.

Next, we substitute the temporally discretized variables (50a-d) into equation (49), perform all necessary convolution integrals in closed form, set all variations at $t = 0$ to zero while allowing the variations at $t = \Delta t$ to remain arbitrary, multiply through by $4 / \Delta t$, and collect like terms to arrive at the following symmetric set of equations:

$$\begin{aligned} & \frac{4}{(\Delta t)^2} \begin{bmatrix} \mathbf{M}_{uu} & \frac{\Delta t}{2} \mathbf{B}_{Ju}^T & -\frac{\Delta t}{2} \mathbf{B}_{\theta u}^T & 0 \\ \frac{\Delta t}{2} \mathbf{B}_{Ju} & -\mathbf{A}_{JJ} & 0 & 0 \\ -\frac{\Delta t}{2} \mathbf{B}_{\theta u} & 0 & -\mathbf{M}_{\theta\theta} & \frac{\Delta t}{2} \mathbf{B}_{H\theta}^T \\ 0 & 0 & \frac{\Delta t}{2} \mathbf{B}_{H\theta} & \mathbf{A}_{HH1} \end{bmatrix} \begin{Bmatrix} \mathbf{u}_1 \\ \mathbf{J}_1 \\ \boldsymbol{\theta}_1 \\ \mathbf{H}_1 \end{Bmatrix} \\ &= \frac{2}{\Delta t} \begin{Bmatrix} \mathbf{j}_1 + \mathbf{j}_0 \\ 0 \\ -(\boldsymbol{\Psi}_1 + \boldsymbol{\Psi}_0) \\ 0 \end{Bmatrix} + \frac{4}{(\Delta t)^2} \begin{bmatrix} \mathbf{M}_{uu} & -\frac{\Delta t}{2} \mathbf{B}_{Ju}^T & \frac{\Delta t}{2} \mathbf{B}_{\theta u}^T & 0 \\ -\frac{\Delta t}{2} \mathbf{B}_{Ju} & -\mathbf{A}_{JJ} & 0 & 0 \\ \frac{\Delta t}{2} \mathbf{B}_{\theta u} & 0 & -\mathbf{M}_{\theta\theta} & -\frac{\Delta t}{2} \mathbf{B}_{H\theta}^T \\ 0 & 0 & -\frac{\Delta t}{2} \mathbf{B}_{H\theta} & \mathbf{A}_{HH0} \end{bmatrix} \begin{Bmatrix} \mathbf{u}_0 \\ \mathbf{J}_0 \\ \boldsymbol{\theta}_0 \\ \mathbf{H}_0 \end{Bmatrix} \quad (52) \end{aligned}$$

where

$$\mathbf{A}_{HH1} = \mathbf{A}_{HH} + \frac{\Delta t}{2} \mathbf{D}_{HH}; \quad \mathbf{A}_{HH0} = \mathbf{A}_{HH} - \frac{\Delta t}{2} \mathbf{D}_{HH} \quad (53)$$

While we could now use (52) as our final set of equations to solve, there is one more simplification that can be made. Because we chose to interpolate the impulses of stress and heat vectors as element-by-element C^{-1} functions, we have the freedom to condense these variables out at the element level prior to assembling

the global set of equations relating to (52), which can save considerable computation time. Then solving for \mathbf{J}_1 and \mathbf{H}_1 gives us

$$\mathbf{J}_1 = \mathbf{A}_{JJ}^{-1} \left[\frac{\Delta t}{2} \mathbf{B}_{Ju} (\mathbf{u}_1 + \mathbf{u}_0) + \mathbf{A}_{JJ} \mathbf{J}_0 \right] \quad (54a)$$

$$\mathbf{H}_1 = \mathbf{A}_{HH1}^{-1} \left[-\frac{\Delta t}{2} \mathbf{B}_{H\theta} (\boldsymbol{\theta}_1 + \boldsymbol{\theta}_0) + \mathbf{A}_{HH0} \mathbf{H}_0 \right] \quad (54b)$$

and after substituting these relations into (52) and rearranging, we can write the condensed set of equations as

$$\begin{bmatrix} \mathbf{K}_{uu1}^e & \mathbf{K}_{u\theta1}^e \\ \mathbf{K}_{\theta u1}^e & \mathbf{K}_{\theta\theta1}^e \end{bmatrix} \begin{Bmatrix} \mathbf{u}_1 \\ \boldsymbol{\theta}_1 \end{Bmatrix} = \begin{Bmatrix} \mathbf{f}_{u1}^e \\ \mathbf{f}_{\theta1}^e \end{Bmatrix} \quad (55)$$

where

$$\mathbf{K}_{uu1}^e = \mathbf{B}_{Ju}^T \mathbf{A}_{JJ}^{-1} \mathbf{B}_{Ju} + \frac{4}{(\Delta t)^2} \mathbf{M}_{uu}; \quad \mathbf{K}_{u\theta0}^e = \mathbf{B}_{Ju}^T \mathbf{A}_{JJ}^{-1} \mathbf{B}_{Ju} - \frac{4}{(\Delta t)^2} \mathbf{M}_{uu} \quad (56a)$$

$$\mathbf{K}_{\theta\theta1}^e = -\mathbf{B}_{H\theta}^T \mathbf{A}_{HH1}^{-1} \mathbf{B}_{H\theta} - \frac{4}{(\Delta t)^2} \mathbf{M}_{\theta\theta}; \quad \mathbf{K}_{\theta\theta0}^e = -\mathbf{B}_{H\theta}^T \mathbf{A}_{HH1}^{-1} \mathbf{B}_{H\theta} + \frac{4}{(\Delta t)^2} \mathbf{M}_{\theta\theta} \quad (56b)$$

$$\mathbf{K}_{u\theta1}^e = \mathbf{K}_{u\theta0}^e = \mathbf{K}_{\theta u1}^{eT} = \mathbf{K}_{\theta u0}^{eT} = -\frac{2}{\Delta t} \mathbf{B}_{\theta u}^T \quad (56c)$$

$$\mathbf{f}_{u1}^e = \frac{2}{\Delta t} (\mathbf{j}_1 + \mathbf{j}_0) - \mathbf{K}_{uu0}^e \mathbf{u}_0 - \mathbf{K}_{u\theta0}^e \boldsymbol{\theta}_0 - \frac{4}{\Delta t} \mathbf{B}_{Ju}^T \mathbf{J}_0 \quad (56d)$$

$$\mathbf{f}_{\theta1}^e = \frac{2}{\Delta t} (\boldsymbol{\Psi}_1 + \boldsymbol{\Psi}_0) - \mathbf{K}_{\theta\theta0}^e \boldsymbol{\theta}_0 - \mathbf{K}_{\theta u0}^e \mathbf{u}_0 - \frac{4}{\Delta t} \mathbf{B}_{H\theta0}^T \mathbf{H}_0 \quad (56e)$$

and

$$\mathbf{B}_{H\theta0}^T = \frac{1}{2} (\mathbf{B}_{H\theta}^T + \mathbf{B}_{H\theta}^T \mathbf{A}_{HH1}^{-1} \mathbf{A}_{HH0}) \mathbf{H}_0 \quad (56f)$$

While all of this has been formulated on the element level, in practice we actually wish to solve the following global set of equations that can be arrived at via standard assembly procedures (Bathe, 1996; Zienkiewicz and Taylor, 2000):

$$\begin{bmatrix} \mathbf{K}_{uu1} & \mathbf{K}_{u\theta1} \\ \mathbf{K}_{\theta u1} & \mathbf{K}_{\theta\theta1} \end{bmatrix} \begin{Bmatrix} \mathbf{u}_n \\ \boldsymbol{\theta}_n \end{Bmatrix} = \begin{Bmatrix} \mathbf{f}_{un} \\ \mathbf{f}_{\theta n} \end{Bmatrix} \quad (57)$$

where \mathbf{u}_n and θ_n consist of all nodal displacements and temperature impulses, respectively, at each time step n . Then one simply needs to first compute the global stiffness \mathbf{K} matrices, specify allowable initial conditions, and then march the solution in time by computing the right hand side at each time step and solving (57).

The formulation defined above is a true space-time finite element method for generalized dynamic thermoelasticity. The temporal discretization is based upon a consistent variational approach for the fully coupled problem. However, it is interesting to examine special cases of this formulation for the classical problems of elastodynamics and heat conduction. For pure elastodynamics, the formulation defined above reduces precisely to the Newmark constant average acceleration method (Dargush et al., 2015). On the other hand, for the problem of heat conduction based upon the classical Fourier law, the mixed convolved action formulation defined above reduces to the Crank and Nicolson (1947) method, except that the primary variable here is the impulse of temperature, rather than the temperature itself (Dargush et al., 2016). For the more general case of dynamic thermoelasticity, the mixed convolved action temporal discretization adjusts between these two extremes depending upon the material parameters governing the conservative and dissipative processes.

6. Computational example problems

We now turn to consider two computational examples to validate the mixed convolved action finite element formulation for dynamic thermoelasticity and to investigate the transient response with and without second sound effects.

6.1 Half-space subject to heat pulses

For this first example we analyze the problem of a spatially uniform heat pulse acting on the free surface of an isotropic half-space. Figure 4 shows a depiction of the half-space problem and Fig. 5 provides a

schematic of the actual domain used for analysis. This finite domain is divided into 1260 triangular elements with biased refinement towards the free surface. Elements have approximate edge nondimensional lengths of 0.02 close to the free surface and 0.2 close to the fixed right side boundary. All material properties are considered to be dimensionless, as well, having values of $\rho_o = 1$, $c_e = 1$, $k = 1$, $E = 0.743$, $\nu = 0.3$, and $\alpha = 0.541$. Various values of second sound relaxation time τ_o and initial temperature T_o are considered. Dimensionless time steps of duration $\Delta t = 0.01$ are used for all analyses. For mechanical boundary conditions, we consider a free (tractionless) surface at $x = 0$ and all other surfaces to be on smooth rollers. For the thermal boundary conditions, a single surface heat pulse is applied to the free surface at $t = 0$, while the other surfaces are considered to be insulated.

In the first case we consider the applied heat pulse to be a half sine-pulse in time, such that $\bar{q}(t) = \sin(\pi t)$ for $0 \leq t \leq 1$. Figures 6a and 6b show the resulting temperature change T and horizontal displacement u_x versus time at $x = 1$, respectively, for the uncoupled case with no second sound effects, and then the coupled case with second sound effects. Note that the strength of the coupling here can be controlled by adjusting T_o . When $T_o \ll 1$, the strain rate dependent coupling term in our formulation becomes negligible, which is referred to somewhat ambiguously as “uncoupled”. For the uncoupled cases in the plots we use $T_o = 1 \times 10^{-6}$. Included in Figs. 6a and 6b are solutions from a well-established boundary element method (Chen and Dargush, 1995) and there is clearly good agreement in the solutions from these two distinct formulations.

For the second case we consider the applied heat pulse to be a sine-squared pulse, such that $\bar{q} = \sin^2(\pi t)$ for $0 \leq t \leq 1$. Plotted in Figs. 7a and 7b are the resulting temperature change T and horizontal displacement u_x , respectively, versus time at $x = 1$ for various values of initial temperature T_o and second

sound relaxation time τ_o . Interestingly, from both plots the highest peak corresponds to the lower value of T_o and highest value of second sound relaxation time τ_o .

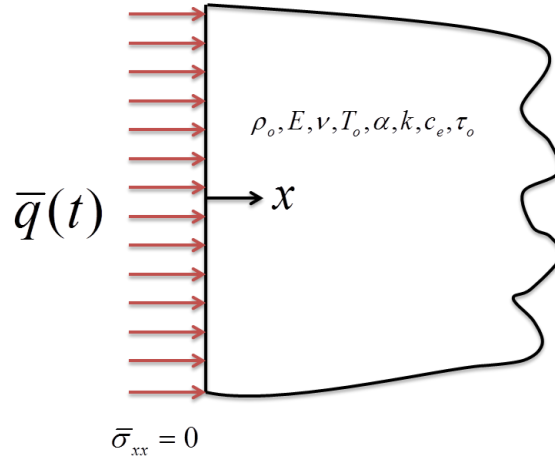


Fig. 4. Thermoelasticity half-space problem definition

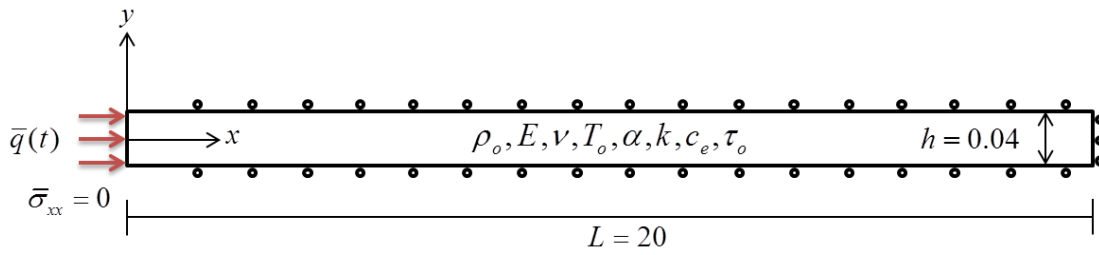


Fig. 5. Thermoelasticity half-space solution domain and boundary conditions

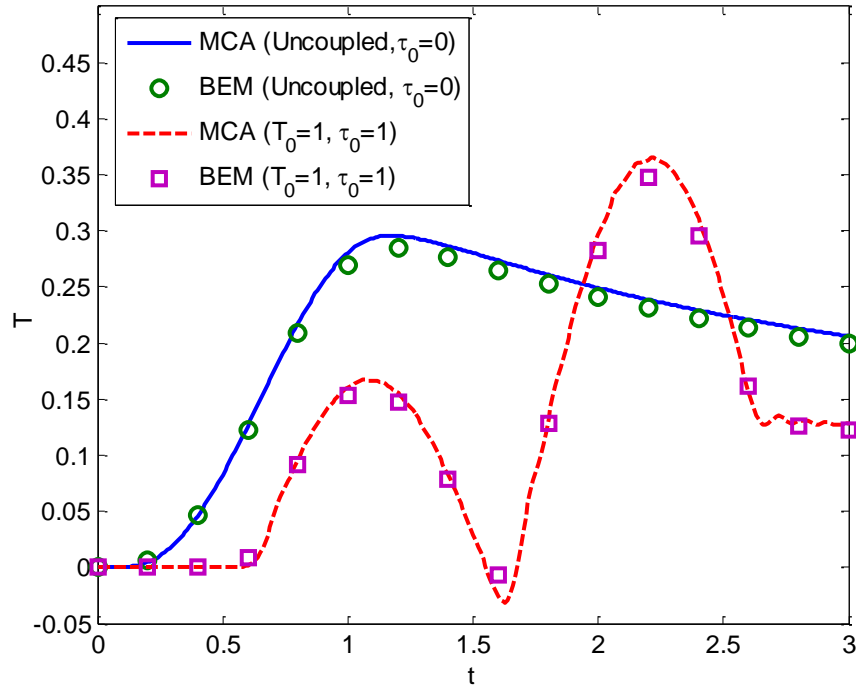


Fig. 6a. Temperature at $x = 1$ versus time for half-sine pulse, MCA and BEM

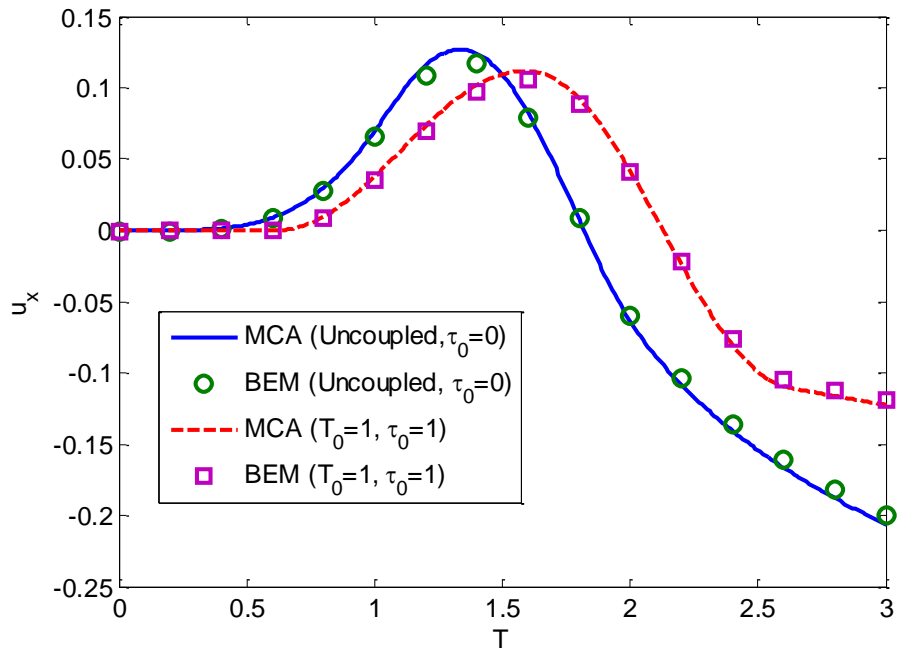


Fig. 6b. Horizontal displacement at $x = 1$ versus time for half-sine pulse, MCA and BEM

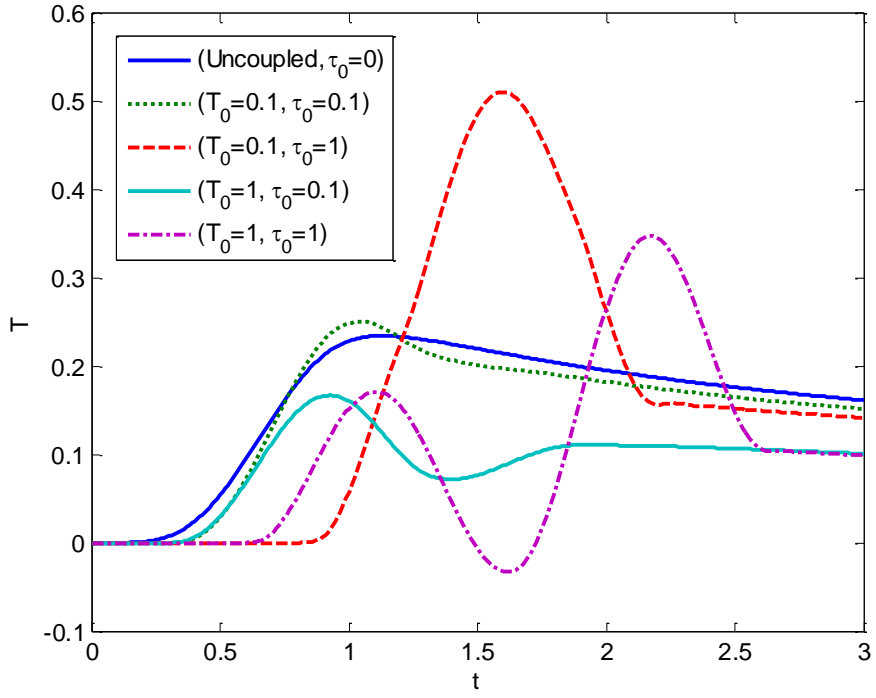


Fig. 7a. Temperature at $x = 1$ versus time for sine-squared pulse

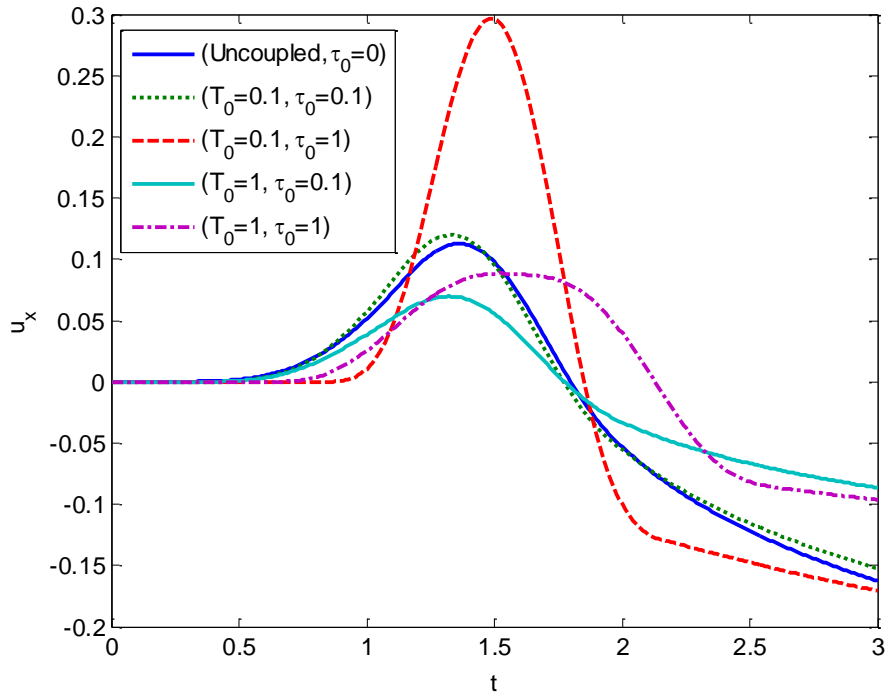


Fig. 7b. Displacement at $x = 1$ versus time for sine-squared pulse

6.2 Square domain with thin surface layer subject to repeated pulse heating

For this example, we consider localized heat flux applied to the center of the top surface of a square domain with a thin top layer, as a simplified model problem for pulsed laser heating. This problem is very similar to the pulse heating problem of Dargush et al. (2016), but here we consider the case with thermoelastic coupling. The square domain is discretized into two sets of 800 uniform triangular elements to assure no biases are introduced. The heat source is spatially triangular, as shown in the problem schematic, and is a square pulse in time. The pulse has time duration $t_d = 0.1$, for which the heat source is “on”. This pulse is applied at the beginning of each period, where the time period is set to $t_p = 1.0$, and then turned “off” for the remainder $t_p - t_d = 0.9$ of each period. The time step for the mixed convolved action numerical analysis is set at $\Delta t = 0.01$ in order to capture the variations in time. The amplitude of the pulse is $q_o = 1$ for all cases. The pulse is applied centrally to the top surface and has width $b = 0.2$. All other surfaces are considered to be insulated, as indicated in Fig. 8. For mechanical boundary conditions we have rollers on all surfaces except for the top, which is traction free.

Dimensionless parameters are considered, with $E = 2$, $\nu = 0$, and unit values for ρ_o , c_e , α and T_o for all cases. We also include second sound effects with relaxation time $\tau_o = 0.1$. The square domain has edge length $L = 2$ and the layer has thickness $h = 0.1$. For the first case we consider the material to have the same isotropic conductivity as the body such that $k_1 = k_2 = 1$, then for case 2 we consider an insulating layer with $k_2 = 0.01$ and for case 3 we consider a conductive layer with $k_2 = 100$.

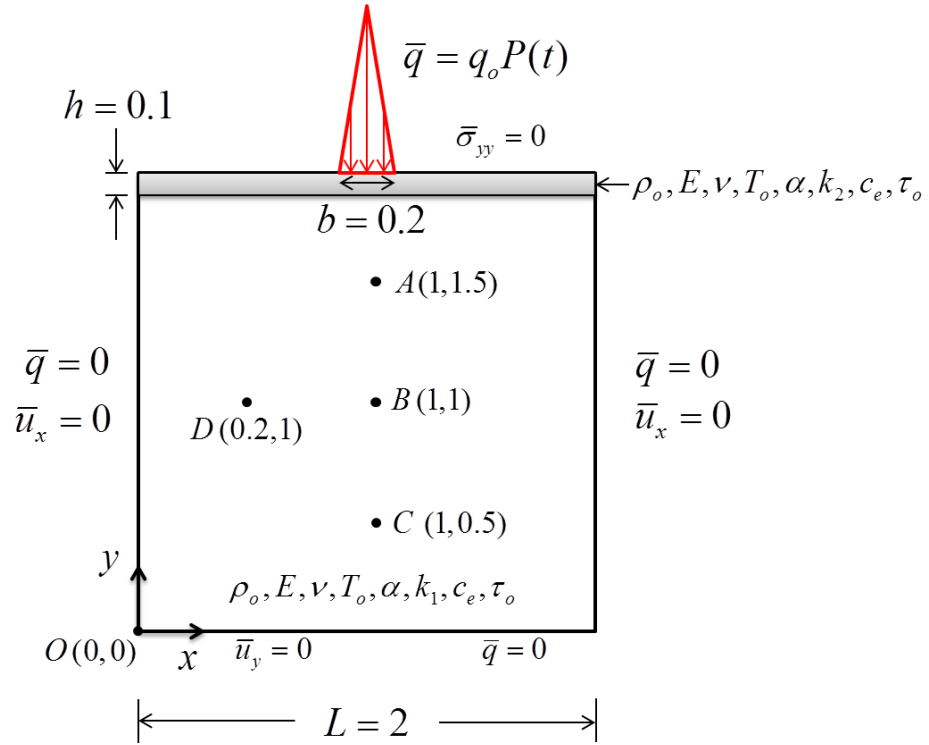


Fig. 8. Thermoelasticity square space problem definition

Figures 9, 10 and 11 show the temperature and vertical displacements plotted against time at points A, B, and C defined in Fig. 8 for layers with the three different levels of thermal conductivity. When compared to the strictly thermal cases analyzed in Dargush et al. (2016), we instantly recognize a significant change in the temperature solution due to coupling. Here the value $\alpha = 1$ is used intentionally to highlight the thermomechanical effects. The consequence of the insulating layer is again to smooth out the second sound effects, however significant oscillations in the thermal field still remain due to the coupling with the elastic stress field. From Figs. 10a and 10b we see that there is indeed a thermal shielding behavior associated with the insulating layer, which is due to the smoothing of the oscillations caused by second sound effects. Comparing Figs. 9, 10 and 11, we see that the conductivity of the layer has little influence on the magnitudes of the vertical displacements, however for the conducting layer we notice less temporal oscillations, which

is likely due to the waves becoming increasingly one-dimensional for layers with increasing thermal conductivity, resulting in less interference.

This transition from 2-d to 1-d response with increasing conductivity of the layer is actually quite interesting and the point of Fig. 12 is to show this transition quantitatively. In Fig. 12 we plot the maximum absolute value of the horizontal displacement $|u_x|$ at point D, as defined in Fig. 8, resulting from a single heat pulse versus layer thermal conductivity k_2 . From this plot we see that for $k_2 > 10k_1$ we have linearly decreasing horizontal displacement. For $k_2 \leq k_1$ we have that the vertical and horizontal displacements are of similar magnitude, while for $k_2 \gg k_1$ the horizontal elastic quantities become negligible and the problem can be considered essentially one-dimensional with evenly distributed heating on the interface. Then although the layer is subject to a highly localized heat source, the rest of the body behaves as though it is subject to a spatially uniform distributed heat source.

Of course it is visually more interesting here to view the dynamic response of the field through a contour plot, rather than by observing the behavior at a single point. In order to capture the full dynamic response, videos of temperature and vertical displacement response, corresponding to all cases examined in this section, are included as supplemental files to this paper. The file names indicate either temperature (temp) or displacement (uy) content, along with the value of k_2 . In addition, Figure 13 provides four sample contour plots that represent a snap shot of these videos at $t = 4.1$, or just after the final applied heat pulse, for the case of no layer ($k_2 = k_1 = 1$) and a highly conductive layer ($k_2 = 10,000$). One should be careful to note that when viewing these contours and videos, the limits of the color scales have been adjusted for each plot to correlate approximately to the minimum and maximum values attained during the 5 second simulation interval for each case.

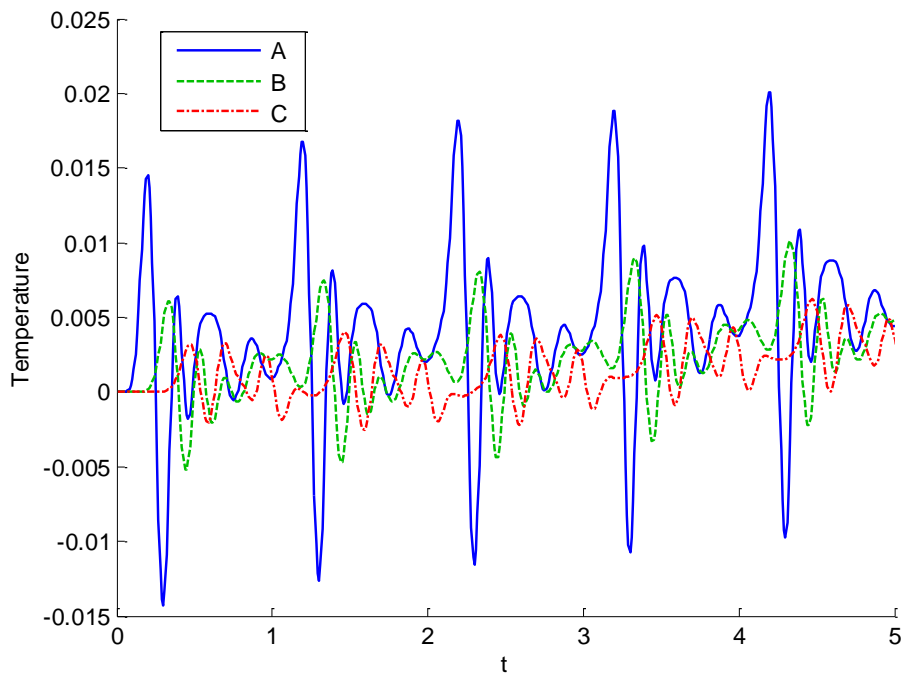


Fig. 9a. Temperature versus time for $k_1 = k_2 = 1$

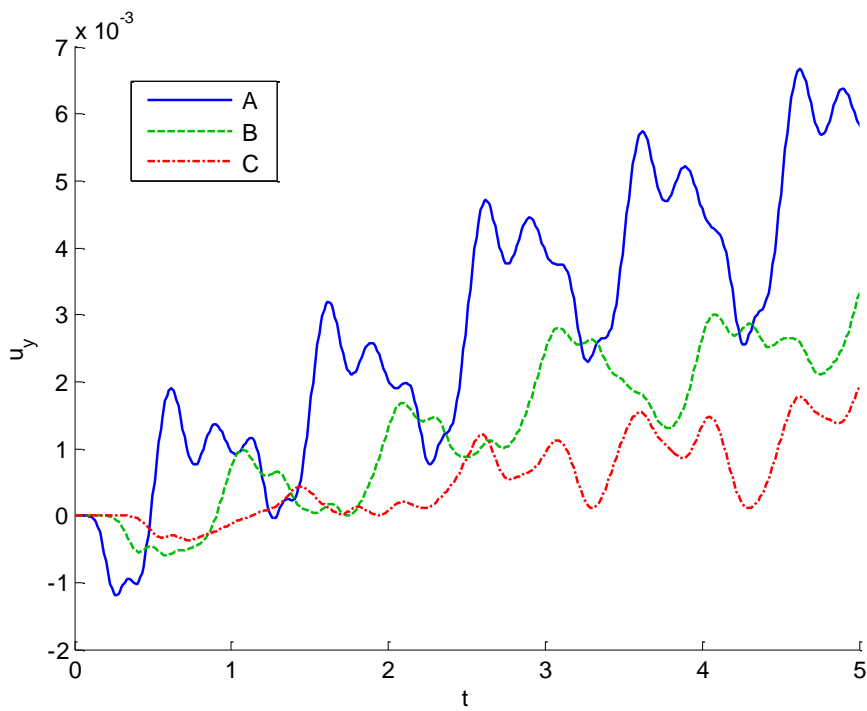


Fig. 9b. Vertical displacement versus time for $k_1 = k_2 = 1$

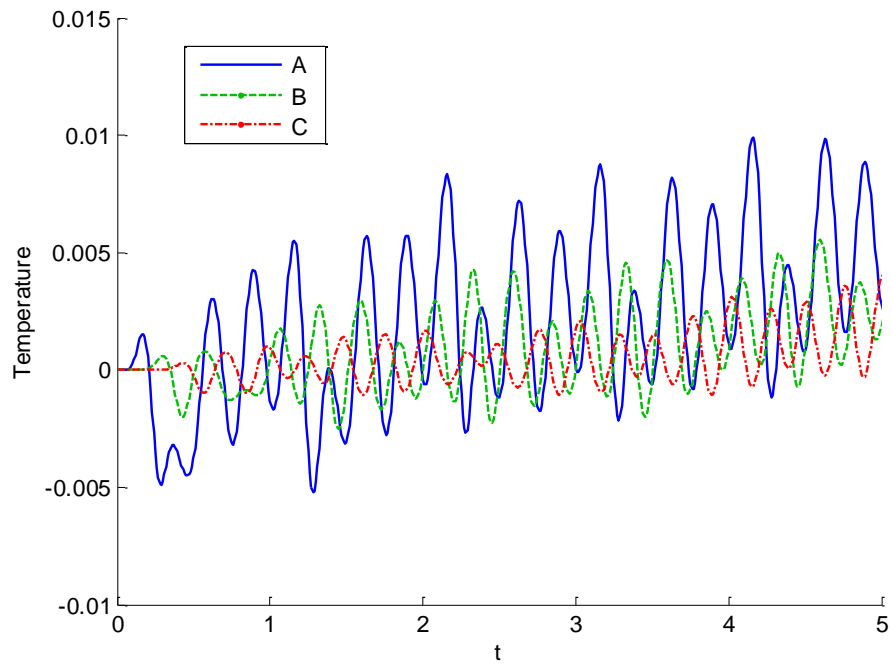


Fig. 10a. Temperature versus time for $k_1 = 1, k_2 = 0.01$

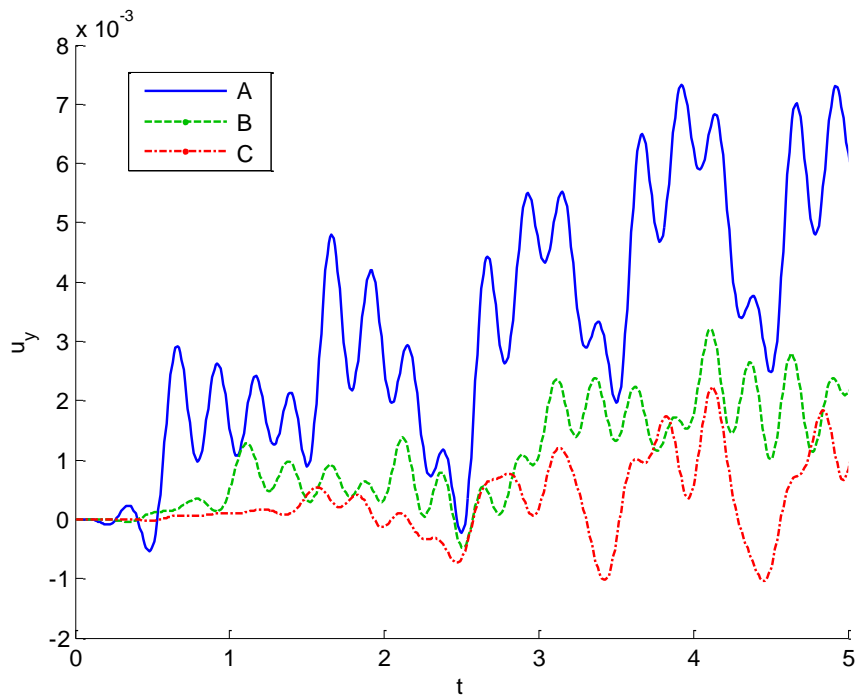


Fig. 10b. Vertical displacement versus time for $k_1 = 1, k_2 = 0.01$

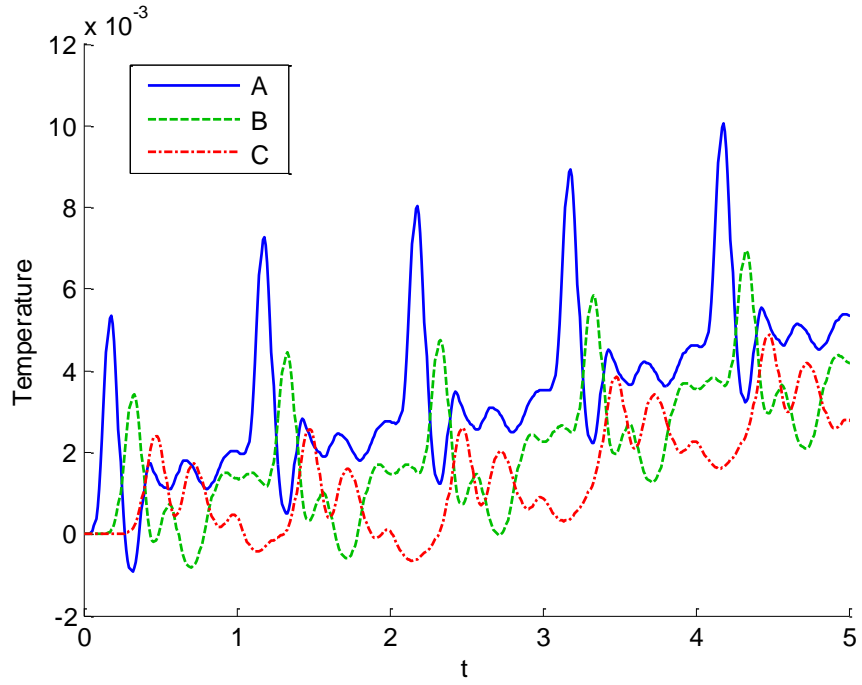


Fig. 11a. Temperature versus time for $k_1 = 1, k_2 = 100$

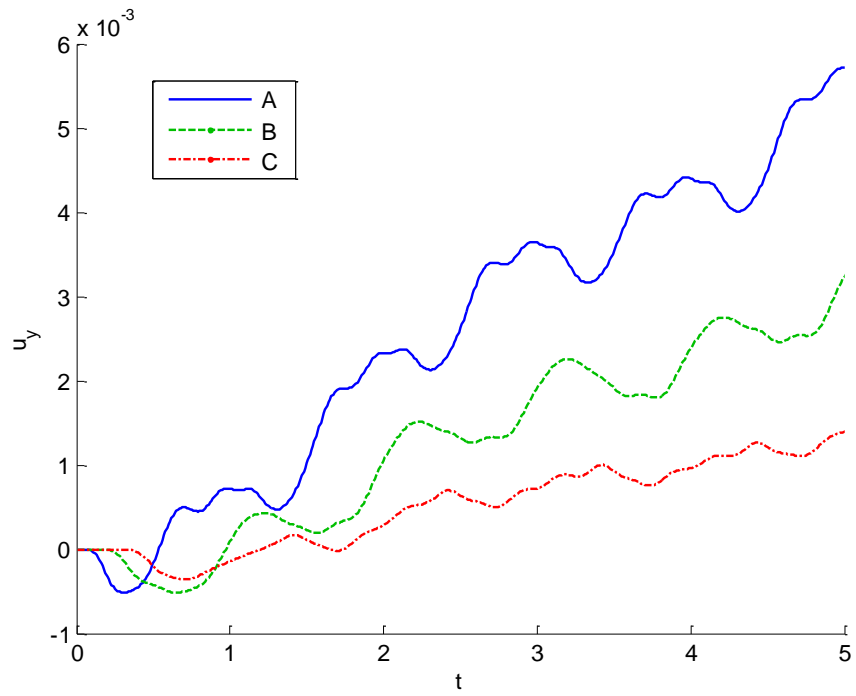


Fig. 11b. Vertical displacement versus time for $k_1 = 1, k_2 = 100$

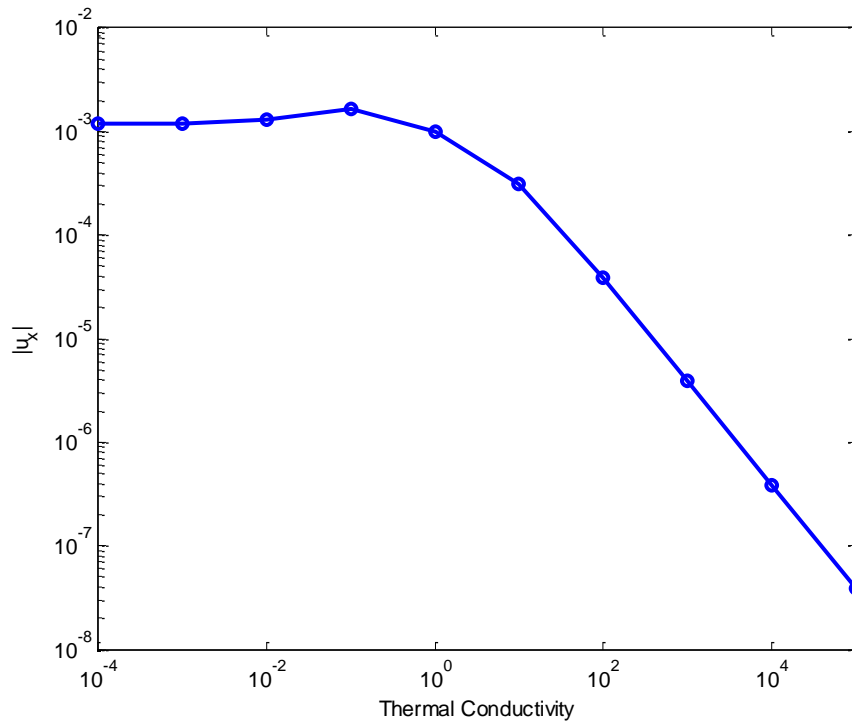


Fig. 12. Maximum horizontal displacement at point D versus layer conductivity k_2

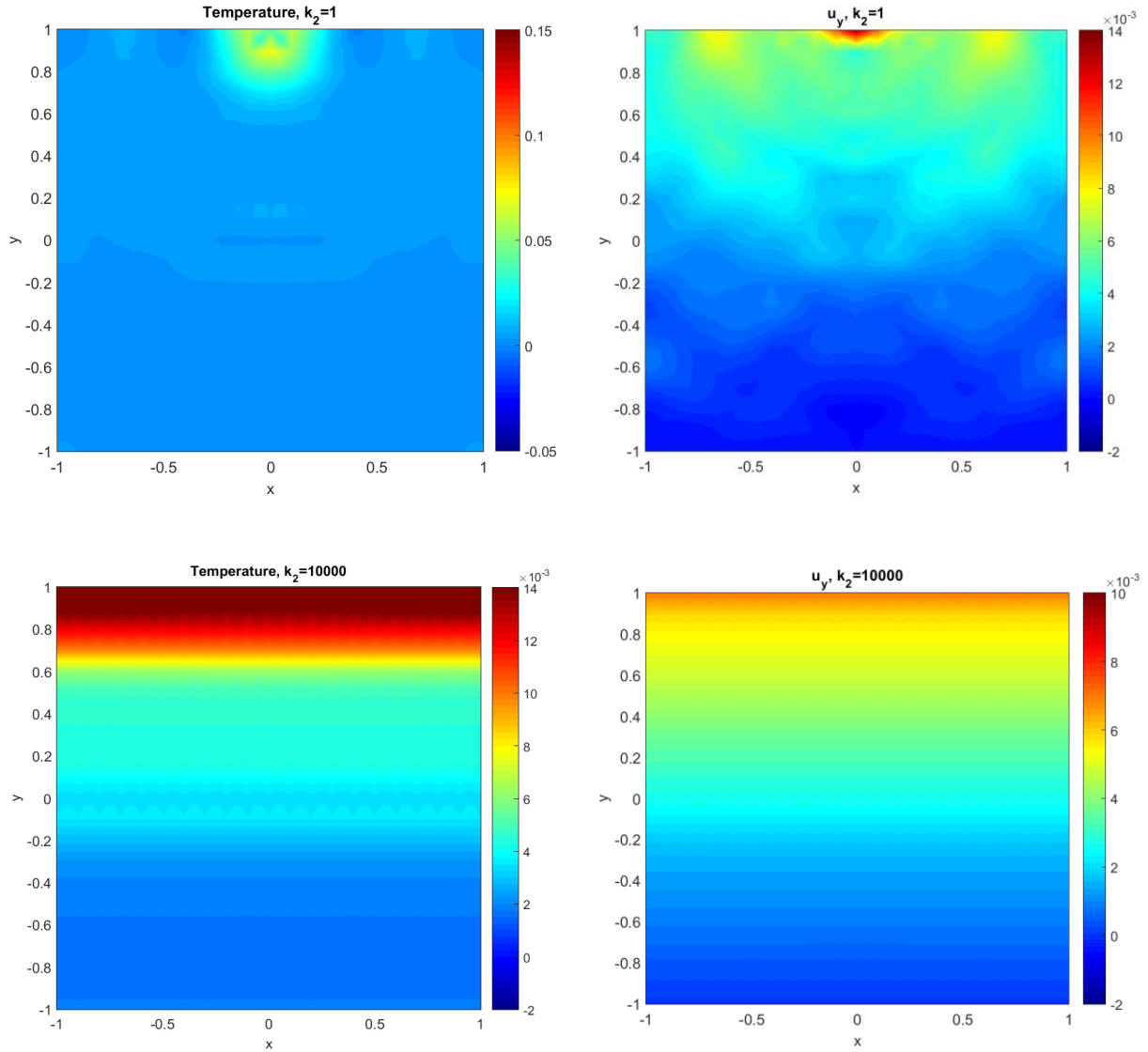


Fig. 13. Sample contour plots of temperature field and vertical displacement at $t = 4.1$: Upper plots for uniform domain with $k_2 = 1$; Lower plots for highly conductive layer with $k_2 = 10000$

7. Conclusions

In the present work, we applied the idea of mixed convolved action for the first time to a multi-physics problem, here associated with coupled dynamic thermoelastic continua. To motivate the development of that action for the continuum case, we first considered a lumped parameter thermoelastic model, for which a systematic derivation was presented. Then, with that process firmly established, the corresponding

continuum problem was addressed by proposing a pure variational time-domain formulation of a new *Principle of Stationary Mixed Convolved Action*. Remarkably, this variational statement produces all of the governing partial differential equations, boundary conditions and initial conditions as its Euler-Lagrange equations. In addition, the variations are taken in a manner that is completely consistent with the specified boundary and initial conditions.

Furthermore, the weak form proposed in (29) has an elegant structure, featuring a balanced appearance of the primary variables and variations, as well as the temporal and spatial derivatives. Here we considered the simplest finite element representation in both time and space, by implementing linear finite elements for temporal discretization, and linear triangular elements for spatial discretization. Of course with the variational framework that the mixed convolved action provides it is simple to create more sophisticated numerical methods with higher order convergence characteristics, even if just by implementing higher order elements.

Several computational examples also were considered to validate the methodology and numerical implementation and to explore aspects of dynamic thermoelasticity with and without second sound effects. In the first example, which reduces to one-dimensional behavior, the mixed convolved action finite element results were compared with an existing boundary element formulation and found to be in excellent agreement. The second example involves the pulsed localized heating of a thin layer positioned over a square domain. Depending upon the relative conductivity of the layer, the temperature and displacement subsurface responses can be quite different. Interestingly, for the case of a highly conducting layer, the solutions reduce to nearly one-dimensional response, despite the spatially localized nature of the applied surface heat source. While this is an idealized example, some insight into related problems of laser-pulsed heating may be possible.

Acknowledgments

This paper is based upon work by the first author supported by the U.S. National Science Foundation (NSF) Graduate Research Fellowship under grant number 1010210. The authors also gratefully acknowledge support for early portions of this work from NSF under grant number CMMI-0900338. The results presented here express the opinion of the authors and not necessarily that of the sponsor.

References

- Apostolakis, G., Dargush, G. F., 2012. Mixed Lagrangian formulation for linear thermoelastic response of structures. *Journal of Engineering Mechanics, ASCE* 138, 508-518.
- Apostolakis, G., Dargush, G. F., 2013. Mixed variational principles for dynamic response of thermoelastic and poroelastic continua. *International Journal of Solids and Structures* 50, 1253-1265.
- Bathe, K.J., 1996. *Finite Element Procedures*. Prentice Hall, Englewood Cliffs, NJ.
- Beris, A. N., Edwards, B. J., 1994. *Thermodynamics of Flowing Systems with Internal Microstructure*. Oxford University Press, New York, NY.
- Biot, M. A., 1955. Variational principles in irreversible thermodynamics with application to viscoelasticity. *Physical Review* 97, 1463-1469.
- Biot, M.A., 1956. Thermoelasticity and irreversible thermodynamics. *Journal of Applied Physics* 27, 240-253.
- Biot, M.A., 1959. New thermomechanical reciprocity relations with application to thermal stress analysis. *Journal of Aero/Space Sciences* 26, 401-408.
- Boley, B.A., Weiner, J.H., 1960. *Theory of Thermal Stresses*. Wiley, New York, NY.
- Brezis, H., Ekeland, I., 1976. Un principe variationnel associe a certaines equations paraboliques. Le case independent du temps. *Comptes Rendus de l'Academie des Sciences Paris* 282, 971-974.
- Buliga, M., De Saxcé, G., 2017. A symplectic Brezis–Ekeland–Nayroles principle. *Mathematics and Mechanics of Solids* 22, 1288–1302.
- Chen, J., Dargush, G.F., 1995. Boundary-element method for dynamic poroelastic and thermoelastic analyses. *International Journal of Solids and Structures* 32, 2257-2278.
- Chen, P.J., Gurtin, M.E., 1968. On a theory of heat conduction involving two temperatures, *Zeitschrift für angewandte Mathematik und Physik* 19, 614–627.
- Chester, M., 1963. Second sound in solids. *Physical Review* 131, 2013-2015.

- Crank, J., Nicolson, P., 1947. A practical method for numerical evaluation of solutions of partial differential equations of the heat conduction type, *Proceedings of the Cambridge Philosophical Society* 43, 50–67.
- Dargush, G.F., Kim, J., 2012. Mixed convolved action. *Physical Review E* 85, 066606.
- Dargush, G.F., 2012. Mixed convolved action for classical and fractional-derivative dissipative dynamical systems. *Physical Review E* 86, 066606.
- Dargush, G.F., Darrall, B.T., Kim, J., Apostolakis, G., 2015. Mixed convolved action principles in linear continuum dynamics. *Acta Mechanica* 226, 4111-4137.
- Dargush, G.F., Apostolakis, G., Darrall, B.T., Kim, J., 2016. Mixed convolved action variational principles in heat diffusion. *International Journal of Heat and Mass Transfer* 100, 790–799.
- De Saxcé, G., Feng, Z.Q., 1998. The bipotential method: a constructive approach to design the complete contact law with friction and improved numerical algorithms. *Mathematical and Computer Modelling* 1998; 28, 225–245.
- El-Karamany, A.S., Ezzat, M.A., 2011. Convolutional variational principle, reciprocal and uniqueness theorems in linear fractional two-temperature thermoelasticity. *Journal of Thermal Stresses* 34, 264-284.
- Ezzat, M.A., El-Karamany, A.S., 2012. The uniqueness and reciprocity theorems for generalized thermo-viscoelasticity with two relaxation times. *International Journal of Engineering Science* 40, 1275-1284.
- Gallagher, R.H., Padlog, J, Bijlaard, P.P., 1962. Stress analysis of complex heated shapes. *ARS Journal* 32, 700-707.
- Goldstein, H., 1950. *Classical Mechanics*. Addison-Wesley Press, Cambridge, MA.
- Green, A.E., Lindsay, K.E., 1972. Thermoelasticity. *Journal of Elasticity* 2, 1-7.
- Green, A.E., Naghdi, P.M., 1992. On undamped heat waves in an elastic solid. *Journal of Thermal Stresses* 15, 253-264.
- Green, A.E., Naghdi, P.M., 1993. Thermoelasticity without energy dissipation. *Journal of Elasticity* 31, 189-208.
- Grmela, M., 1984. Bracket formulation of dissipative fluid mechanics equations. *Physics Letters*. 102A, 355-358.
- Grmela, M., 2014. Contact geometry of mesoscopic thermodynamics and dynamics. *Entropy* 16, 1652-1686.
- Grmela, M., 2015. Geometry of multiscale nonequilibrium thermodynamics. *Entropy* 17, 5938-5964.
- Grmela, M., Ottinger, H.C., 1997. Dynamics and thermodynamics of complex fluids. I. Development of a general formalism. *Physical Review E* 56, 6620-6632.

- Gurtin, M.E., 1963. Variational principles in the linear theory of viscoelasticity. *Archive for Rational Mechanics and Analysis* 13, 179-191.
- Gurtin, M.E., 1964a. Variational principles for linear initial-value problems, *Quarterly of Applied Mathematics* 22(3), 252-256.
- Gurtin, M.E., 1964b. Variational principles for linear elastodynamics, *Archive for Rational Mechanics and Analysis* 16(1), 34-50.
- Halphen, B., Nguyen Quoc, S., 1975. Sur les matériaux standard généralisés. *Journal de Mécanique* 14, 39–63.
- Hamilton, W.R., 1834. On a general method in dynamics. *Philosophical Transactions of the Royal Society of London* 124, 247-308.
- Hamilton, W.R., 1835. Second essay on a general method in dynamics. *Philosophical Transactions of the Royal Society of London* 125, 95-144.
- Houlsby, G.T., Puzrin, A.M., 2006. *Principles of Hyperplasticity: An Approach to Plasticity Theory Based on Thermodynamic Principles*. Springer, London.
- Ionescu-Casimer, V., 1964. Problem of linear coupled thermoelasticity. Theorems of reciprocity for the dynamic problem of coupled thermoelasticity. I. *Bulletin de l'Academie Polonaise des Sciences. Serie des Sciences Techniques* 12, 473-488.
- Joseph, D.D., Perziosi, L., 1989. Heat waves. *Reviews of Modern Physics* 61, 41-73.
- Kane, C., Marsden, J.E., Ortiz, M., 1999. Symplectic-energy-momentum preserving variational integrators. *Journal of Mathematical Physics* 40, 3357-3371.
- Kane, C., Marsden, J.E., Ortiz, M., West, M., 2000. Variational integrators and the Newmark algorithm for conservative and dissipative mechanical systems. *International Journal for Numerical Methods in Engineering* 49, 1295-1325.
- Kaufman, A.N., 1984. Dissipative Hamiltonian systems: A unifying principle. *Physics Letters* 100A, 419-422.
- Lanczos, C., 1949. *The Variational Principles of Mechanics*. University of Toronto Press, Toronto.
- Lavan, O., Sivaselvan, M.V., Reinhorn, A.M., Dargush, G.F., 2009. Progressive collapse analysis through strength degradation and fracture in the Mixed Lagrangian Formulation. *Earthquake Engineering & Structural Dynamics* 38, 1483-1504.
- Lavan, O., 2010. Dynamic analysis of gap closing and contact in the Mixed Lagrangian Framework: Toward progressive collapse prediction. *Journal of Engineering Mechanics, ASCE* 136, 979-986.
- Lord, H.W., Shulman, Y., 1967. A generalized dynamical theory of thermoelasticity. *Journal of the Mechanics and Physics of Solids* 15, 299-309.
- Lotfian, Z., Sivaselvan, M.V., 2014. A projected Newton algorithm for the dual convex program of elastoplasticity. *International Journal for Numerical Methods in Engineering* 97, 903–936.

- Marsden, J.E., Ratiu, T.S., 1994. *Introduction to Mechanics and Symmetry: A Basic Exposition of Classical Mechanical Systems*. Springer-Verlag, New York, NY.
- Marsden, J.E., West, M., 2001. Discrete mechanics and variational integrators. *Acta Numerica* 10, 357-514.
- Morrison, P.J., 1984. Bracket formulation for irreversible classical fields. *Physics Letters* 100A, 423-427.
- Morse, P.M., Feshbach, H., 1953. *Methods of Theoretical Physics*. McGraw-Hill, New York, NY.
- Nayroles, M.B., 1976. Deux theoremes de minimum pour certains systemes dissipatifs. *Comptes Rendus de l'Academie des Sciences Paris* 282, A1035–A1038.
- Nickell, R.E., Sackman, J.L., 1968. Approximate solutions in linear, coupled thermoelasticity. *Journal of Applied Mechanics* 35, 255-266.
- Nowacki, W., 1986. *Thermoelasticity*. Pergamon Press, Warsaw.
- Oden, J.T., Reddy, J.N., 1983. *Variational Methods in Theoretical Mechanics*. Springer-Verlag, Berlin.
- Ottinger, H.C., Grmela, M., 1997. Dynamics and thermodynamics of complex fluids. II. Illustrations of a general formalism. *Physical Review E* 56, 6633-6655.
- Prevost, J.H., Tao, D., 1983. Finite element analysis of dynamic coupled thermoelasticity problems with relaxation times. *Journal of Applied Mechanics* 50, 817-822.
- Rayleigh, J.W.S., 1877. *The Theory of Sound. I & II*. Second edition, reprint in 1945. Dover Publications, New York, NY.
- Riewe, F., 1996. Nonconservative Lagrangian and Hamiltonian mechanics. *Physical Review E* 53, 1890-1899.
- Riewe, F., 1997. Mechanics with fractional derivatives. *Physical Review E* 55, 3581-3592.
- Sherief, H.H., El-Sayed, A.M.A., Abd El-Latief, A.M., 2010. Fractional order theory of thermoelasticity. *International Journal of Solids and Structures* 47, 269–275.
- Sivaselvan, M.V., Reinhorn, A.M., 2006. Lagrangian approach to structural collapse simulation. *Journal of Engineering Mechanics, ASCE* 132, 795-805.
- Sivaselvan, M.V., Lavan, O., Dargush, G.F., Kurino, H., Hyodo, Y., Fukuda, R., Sato, K., Apostolakis, G., Reinhorn, A.M., 2009. Numerical collapse simulation of large-scale structural systems using an optimization-based algorithm. *Earthquake Engineering and Structural Dynamics* 38, 655-677.
- Tonti, E., 1973. On the variational formulation for linear initial value problems. *Annali di Matematica Pura ed Applicata* XCV, 331-360.
- Tonti, E., 1985. Inverse problem: Its general solution. In: *Differential Geometry, Calculus of Variations and Their Applications*, Ed: G. M. Rassias, T. M. Rassias, Marcel Dekker, New York, NY.

Wilson, E.L., Nickell, R.E., 1966. Application of the finite element method to heat conduction analysis. Nuclear Engineering and Design 4, 276-286.

Zienkiewicz, O.C., Taylor, R.L., 2000. The Finite Element Method. Butterworth-Heinemann, Oxford.